ELSEVIER

Comput. Methods Appl. Mech. Engrg. 162 (1998) 49–78

Computer methods in applied mechanics and engineering

Uniformly convergent finite element methods for singularly perturbed elliptic boundary value problems: convection–diffusion type

Jichun Li, I.M. Navon*

Department of Mathematics and Supercomputer Computations Research Institute, Florida State University, Tallahassee, FL 32306-4052, USA

Received 8 July 1997

Abstract

In this paper we consider the standard bilinear finite element method (FEM) and the corresponding streamline diffusion FEM for the singularly perturbed elliptic boundary value problem $-\varepsilon^{\alpha}(\partial^2 u/\partial x^2 + \partial^2 u/\partial y^2) - b(x, y)\cdot\nabla u + a^{\alpha}(x, y)u = f(x, y)$ in the two space dimensions. By using the asymptotic expansion method of Vishik and Lyusternik [36] and the technique we used in [21,22], we prove that the standard bilinear FEM on a Shishkin type mesh achieves first-order uniform convergence rate globally in L^2 norm for both the ordinary exponential boundary layer case and the parabolic boundary layer case. Extensive numerical results are carried out for both cases. The results show that our methods perform much better than either the classical standard or streamline diffusion FEM.

Introduction

In this paper, we consider some finite element methods for the singularly perturbed elliptic boundary value problem:

$$-\varepsilon^{\alpha}\left(\frac{\partial^2 u}{\partial x^2}+\frac{\partial^2 u}{\partial y^2}\right) - b(x, y)\cdot\nabla u + a^{\alpha}(x, y)u = f(x, y) \quad \text{in } \Omega \equiv (0, 1)\times(0, 1)\,, \tag{1}$$

$$u = 0 \quad \text{on } \partial\Omega\,, \tag{2}$$

where $\varepsilon \in (0,1]$ is a small positive parameter and $\alpha = 1$ or 2.

This problem is a very extensively discussed model for singularly perturbed problems [8,35,36,37]. Also, this problem is used quite often for testing numerical solvers (cf. Bank [2] and Hackbusch [12, Ch. 10]). In fluid mechanics, this model problem is related to convection dominated flows. It arises in many areas, such as fluid flow in water resources; oil and gas reservoir simulation; and in heat and mass transfer in chemical and nuclear engineering. There is a large number of different methods devoted to this model problem and its corresponding one space dimension versions. Finite difference methods are discussed in [9,13,26], while finite volume methods are discussed in [23]. In the context of the finite element method, there is a variety of approaches, such as Petrov–Galerkin FEM [15], Streamline Diffusion FEM [17,18,39], High-order FEM [1,14] and Adaptive FEM [7], to name but a few. For more details, see Hughes [16], Carey and Oden [6, Ch. 5] and Zienkiewicz and

* Corresponding author. E-mail: navon@scri.fsu.edu

0045-7825/98/$19.00
PII: S0045-7825(97)00329-0

Taylor [38, Ch. 12]. However, few of the above methods are globally uniformly convergent (GUC); that is, the error between the original continuous solution u and the computed FEM solution u_h satisfies:

$$\|u - u_h\|_\varepsilon \leq Ch^m$$

for some positive constant C that is independent of ε and of the mesh size. More details about GUC methods can be found in [26,30].

It is well known [17] that both the standard FEM and streamline diffusion FEM generally have the following global error estimates

$$\|\!|u - u_h|\!\|_\Omega \leq Ch^m \|u\|_{H^n(\Omega)},$$

where $H^n(\Omega)$ for n a positive integer denotes the usual Sobolev space [3] with norm $\|\cdot\|_{H^n(\Omega)}$ and $\|\!|\cdot|\!\|_\Omega$ denotes an energy norm on Ω. But since ε is usually very small for this type problem, there exist very sharp boundary layers or internal layers [10,41,42]. And usually, $\|u\|_{H^n(\Omega)} \leq C\varepsilon^{-k}$, where k is some positive integer. Hence, to ensure global convergence, the mesh size h must be less than or equal to ε^p, where p is a positive number, which is impossible in practice, since usually ε can be as small as 10^{-10}. Hence, much work switched to local error analysis (cf. Johnson et al. [18], Zhou and Rannacher [39] and for more details see Wahlbin [37]).

In the following, we will focus on GUC methods achieved by FEM. It is well known that uniform convergence can be achieved by using exponentially fitted splines or combinations with other functions as trial and test space [27,30]. However, they are complicated to use and have very low convergence rate, which is $\|u - u_h\|_\varepsilon \leq ch^{1/2}$, where $\|\cdot\|_\varepsilon$ is a variant of an energy norm. Another type of uniform convergence is achieved by using hp FEM [33], which is also very complicated and is still under development. Recently, almost optimal uniform convergence results were achieved for ordinary differential equations and parabolic equations by using the standard Galerkin or streamline diffusion FEM on a Shishkin type mesh [11,19,30]. The Shishkin type mesh is a piecewise uniform mesh, which specifies a fine uniform mesh inside part but not all of the boundary layer and coarse uniform mesh elsewhere a priori, yet still gives convergence that is uniform in ε. It is very easy to apply, but the aforementioned studies were restricted only in one space dimension. Recently, Madden et al. [24] carried out some computational experiments for FEM on Shishkin meshes in two dimensions, and their results seemed very promising. However no theoretical analysis efforts were carried out as yet. Just as Roos et al. said in [30]: "Finite element methods that use Shishkin meshes in two or more dimensions have not been explored in the literature." Up to now, to the best of our knowledge, except for our first attempt applied for the reaction-diffusion type problem [21,22], the theoretical analysis for FEM on Shishkin meshes in two space dimensions is still missing.

This paper constitutes another attempt in the above mentioned area. We prove here by using the asymptotic expansion method of Vishik and Lyusternik [36] (see also [8,35]) and the technique we used in [22], that the standard bilinear FEM on a Shishkin type mesh achieves first-order uniform convergence rate globally in L^2 norm for both the ordinary exponential boundary layer case and the parabolic boundary layer case. Extensive numerical tests are carried out for both cases. We also present a brief discussion for the streamline diffusion methods on these Shishkin type meshes. Numerical results are also presented for comparisons between our methods and the classical standard and streamline diffusion FEM. The results show that our methods are much better than either the classical standard or the streamline diffusion FEM.

The organization of this paper is as follows. In Section 2, we discuss the pure exponential boundary layer case, where we assume $\alpha = 1$ and b_1, b_2 and a are positive constants. Then in Section 3, we discuss the more complicated parabolic boundary layer case, where we take $\alpha = 2$, $b_1 = 0$, and $b_2 > 0$. Finally, extensive numerical results for both cases are provided and discussed in Section 4.

Through this paper we shall use C, sometimes subscripted, to denote a generic positive constant that is independent of both ε and the mesh. Also, we use $(\cdot)_x$ to denote the derivative with respect to the variable x.

2. Exponential boundary layer case

In this section we consider the following problem:

$$L_\varepsilon u \equiv -\varepsilon\left(\frac{\partial^2 u}{\partial x^2} + \frac{\partial^2 u}{\partial y^2}\right) - b \cdot \nabla u + au = f(x, y) \quad \text{in } \Omega, \tag{3}$$

$$u = 0 \quad \text{on } \partial\Omega, \tag{4}$$

which corresponds to the case of $\alpha = 1$ in (1). To avoid lengthy technicalities, we assume that the coefficients a and $b = (b_1, b_2)$ are positive constants. For variable coefficients, a similar research work can be carried out (cf. [22]).

2.1. Derivative estimates of the solution

In this subsection, we will obtain some derivative estimates for the solution of (3), (4) under the compatibility conditions [27,30]:

$$(H^*) \quad f(0,0) = f(0,1) = f(1,0) = f(1,1) = 0$$

which ensure that the solution of (3), (4) $u(x, y) \in C^4(\Omega) \cap C^2(\bar{\Omega})$, where $\bar{\Omega} = \Omega \cup \partial\Omega$. Such compatibility conditions are necessary for the global pointwise derivative estimates of the solution [27,30]. O'Riordan and Stynes [27] obtained the derivative estimates for a very similar problem. Hence, we just sketch the proof here.

In this section will make repeated use of the following weak maximum principle:

LEMMA 2.1.1. For any functions $w(x, y) \in C^2(\Omega) \cap C^0(\bar{\Omega})$, if $w \geq 0$ on $\partial\Omega$ and $L_\varepsilon w \geq 0$ on Ω, then $w \geq 0$ on $\bar{\Omega}$.

PROOF. It can be proved easily by contradiction (cf. Eckhaus [8, Lemma 6.2.1.1]).

By choosing the barrier functions [22,27] properly, we can obtain the following estimates for the solution u of (3), (4).

LEMMA 2.1.2

(*I*) $|u(x, y)| \leq C(1 - e^{(-2b_1 x)/\varepsilon})$ *on* $\bar{\Omega}$,
(*II*) $|u(x, y)| \leq C(1 - x)$ *on* $\bar{\Omega}$,
(*III*) $|u(x, y)| \leq C(1 - e^{(-2b_2 y)/\varepsilon})$ *on* $\bar{\Omega}$,
(*IV*) $|u(x, y)| \leq C(1 - y)$ *on* $\bar{\Omega}$.

PROOF. (I) Using the barrier function $\phi(x, y) = C(1 - e^{(-2b_1 x)/\varepsilon})$, we have

$$\begin{aligned} L_\varepsilon(\phi \pm u) &= C4b_1^2\varepsilon^{-1} e^{(-2b_1 x)/\varepsilon} - 2b_1^2 C\varepsilon^{-1} e^{(-2b_1 x)/\varepsilon} + aC(1 - e^{(-2b_1 x)/\varepsilon}) \pm f, \\ &= C(2b_1^2\varepsilon^{-1} - a) e^{(-2b_1 x)/\varepsilon} + aC \pm f \\ &\geq 0, \quad \text{for sufficiently large } C, \end{aligned}$$

where we use the fact that ε is very small. Then, from $(\phi \pm u)|_{\partial\Omega} \geq 0$ and Lemma 2.1.1 we conclude our proof.

(II) Use the barrier function $\phi(x, y) = C(1 - x)$.
(III) Use the barrier function $\phi(x, y) = C(1 - e^{(-2b_2 y)/\varepsilon})$.
(IV) Use the barrier function $\phi(x, y) = C(1 - y)$.

LEMMA 2.1.3.

(*I*) $|u_x(x, y)| \leq C\varepsilon^{-1}$ *on* $\partial\Omega$,
(*II*) $|u_y(x, y)| \leq C\varepsilon^{-1}$ *on* $\partial\Omega$.

PROOF. (I) By Lemma 2.1.2(I), we have

$$\begin{aligned} |u_x(0, y)| &= \left| \lim_{x \to 0^+} \frac{u(x, y) - u(0, y)}{x} \right| \leq \lim_{x \to 0^+} \left| \frac{u(x, y) - u(0, y)}{x} \right| \\ &\leq \lim_{x \to 0^+} \frac{C(1 - e^{(-2b_1 x)/\varepsilon})}{x} = \frac{2b_1 C}{\varepsilon}. \end{aligned}$$

Similarly, by Lemma 2.1.2(II), we have

$$|u_x(1, y)| = \left| \lim_{x\to 1^-} \frac{u(1, y) - u(x, y)}{(1-x)} \right| \leqslant \lim_{x\to 1^-} \left| \frac{u(1, y) - u(x, y)}{(1-x)} \right|$$
$$\leqslant \lim_{x\to 1^-} \frac{C(1-x)}{(1-x)} = C .$$

Using the given boundary condition (4), we have $u_x(x, 0) = u_x(x, 1) = 0$, which concludes our proof.
(II) Use a similar proof as in (I) by Lemma 2.1.2(III) and (IV).

LEMMA 2.1.4.
(*I*) $|u_x(x, y)| \leqslant C(1 + \varepsilon^{-1} e^{(-b_1 x)/\varepsilon})$ *on* $\overline{\Omega}$,
(*II*) $|u_y(x, y)| \leqslant C(1 + \varepsilon^{-1} e^{(-b_2 y)/\varepsilon})$ *on* Ω.

PROOF. (I) Consider the barrier function $\phi(x, y) = C(1 + \varepsilon^{-1} e^{(-b_1 x)/\varepsilon})$ then we have

$$L_\varepsilon(\phi \pm u_x) = aC(1 + \varepsilon^{-1} e^{(-b_1 x)/\varepsilon}) \pm f_x$$
$$\geqslant 0 \quad \text{for sufficiently large } C ,$$

and note that $(\phi \pm u_x)|_{\partial\Omega} \geqslant 0$, which concludes our proof of (I).
(II) To prove (II), we use the barrier function $\phi(x, y) = C(1 + \varepsilon^{-1} e^{(-b_2 y)/\varepsilon})$.

LEMMA 2.1.5.
(*I*) $|u_{xx}(x, y)| \leqslant C\varepsilon^{-2}$ *on* $\partial\Omega$
(*II*) $|u_{yy}(x, y)| \leqslant C\varepsilon^{-2}$ *on* $\partial\Omega$.

PROOF. (I) From the boundary condition (4), we have $u_{xx}|_{y=0,1} = 0$. From Eq. (3) and boundary condition (4), we obtain $u_{xx}|_{x=0,1} = -\varepsilon^{-1}(f + b_1 u_x)|_{x=0,1} \leqslant C\varepsilon^{-2}$.
(II) Use a similar proof as in (I).

LEMMA 2.1.6.
(*I*) $|u_{xx}(x, y)| \leqslant C(1 + \varepsilon^{-2} e^{(-b_1 x)/\varepsilon})$ *on* $\overline{\Omega}$,
(*II*) $|u_{yy}(x, y)| \leqslant C(1 + \varepsilon^{-2} e^{(-b_2 y)/\varepsilon})$ *on* Ω.

PROOF. (I) Use the barrier function $\phi(x, y) = C(1 + \varepsilon^{-2} e^{(-b_1 x)/\varepsilon})$, then

$$L_\varepsilon(\phi \pm u_{xx}) = aC(1 + \varepsilon^{-2} e^{(-b_1 x)/\varepsilon}) \pm f_{xx}$$
$$\geqslant 0 \quad \text{for sufficiently large } C .$$

then using $(\phi \pm u_{xx})|_{\partial\Omega} \geqslant 0$ and Lemma 2.1.1 concludes our proof.
(II) Use the barrier function $\phi(x, y) = C(1 + \varepsilon^{-2} e^{(-b_2 y)/\varepsilon})$.

REMARK 2.1. From the above estimates, we can see that the solution exhibits very sharp boundary layers at $x = 0$ and $x = 1$, which can also be seen by carrying out an asymptotic expansion which is presented in the next subsection.

2.2. The asymptotic expansion

In this subsection, we will use the general asymptotic expansion method developed by Vishik and Lyusternik [36] to develop an asymptotic expansion for problem (3), (4). Roos et al. [30, p. 183] sketched its asymptotic expansion very briefly. Here, we will present a more detailed analysis by using the method of Vishik and Lyusternik.

The leading term in the regular part of the asymptotic solution $U(x, y) = \Sigma_{i=0}^{\infty} \varepsilon^i U_i(x, y)$ is defined by

$$-b \cdot \nabla U_0 + aU_0 = f(x, y) \quad \text{in } \Omega$$
$$U_0|_{x=1} = U_0|_{y=1} = 0 .$$

Since the regular part of the asymptotic expansion generally does not satisfy the boundary conditions at $x = 0$ and $y = 0$, we have to introduce the boundary layer functions $V(\xi, y) = \Sigma_{i=0}^{\infty} \varepsilon^i V_i(\xi, y)$ and $W(x, \eta) = \Sigma_{i=0}^{\infty} \varepsilon^i W_i(x, \eta)$ to eliminate the discrepancies at $x = 0$ and $y = 0$, respectively, where $\xi = x/\varepsilon$ and $\eta = y/\varepsilon$.

The first two terms of V satisfy the following ordinary differential equations:

$$(V_0)_{\xi\xi} + b_1(V_0)_{\xi} = 0 , \quad \text{for } \xi > 0$$
$$V_0|_{\xi=0} = -U_0(0, y) , \qquad V_0|_{\xi\to\infty} = 0$$

and

$$(V_1)_{\xi\xi} + b_1(V_1)\xi = b_2(V_0)_y - aV_0 , \quad \text{for } \xi > 0$$
$$V_1|_{\xi=0} = -U_1(0, y) , \qquad V_1|_{\xi\to\infty} = 0 ,$$

respectively. From which we obtain the solution $V_0(\xi, y) = -U_0(0, y)\, e^{-b_1\xi}$.

Similarly, we can obtain $W_0(x, \eta) = -U_0(x, 0)\, e^{-b_2\eta}$.

Note that $u - U - V - W$ is not small near the corner $(0, 0)$ since the boundary layer terms overlay there. We need a corner layer function $Z(\xi, \eta) = \Sigma_{i=0}^{\infty} \varepsilon^i Z_i(\xi, \eta)$, to compensate this discrepancy. The first two terms satisfy the following equations:

$$(Z_0)_{\xi\xi} + (Z_0)_{\eta\eta} + b_1(Z_0)_{\xi} + b_2(Z_0)_{\eta} = 0 , \quad \forall\, \xi > 0, \eta > 0 ,$$
$$Z_0|_{\xi=0} = -(U_0 + V_0 + W_0)|_{\xi=0} , \qquad Z_0|_{\eta=0} = -(U_0 + V_0 + W_0)|_{\eta=0}$$
$$Z_0 \to 0 \quad \text{as } \xi \to \infty, \eta \to \infty .$$

and

$$(Z_1)_{\xi\xi} + (Z_1)_{\eta\eta} + b_1(Z_1)_{\xi} + b_2(Z_1)_{\eta} = aZ_0, \quad \forall \xi > 0, \eta > 0 ,$$
$$Z_1|_{\xi=0} = -(U_1 + V_1 + W_1)|_{\xi=0} , \qquad Z_1|_{\eta=0} = -(U_1 + V_1 + W_1)_{\eta=0}$$
$$Z_1 \to 0 \quad \text{as } \xi \to \infty, \eta \to \infty .$$

from which we obtain $Z_0(\xi, \eta) = U_0(0, 0)\, e^{-b_1\xi}\, e^{-b_2\eta}$.

LEMMA 2.2.1. Let u be the solution of (3), (4) and $U_0 \in C^2(\bar{\Omega})$, then

$$|R(x, y)| \leqslant C\varepsilon , \quad \textit{for all } (x, y) \in \bar{\Omega} \equiv \Omega \cup \partial\Omega ,$$

where $R(x, y) = u(x, y) - u_{as}(x, y)$ denote the remainder in the asymptotic expansion

$$u_{as}(x, y) = U_0(x, y) + V_0(\xi, y) + W_0(x, \eta) + Z_0(\xi, \eta) .$$

PROOF. Consider the auxiliary asymptotic expansion

$$\bar{u}_{as}(x, y) = U_0(x, y) + V_0(\xi, y) + \varepsilon V_1(\xi, y) + W_0(x, \eta) + \varepsilon W_1(x, \eta) + Z_0(\xi, \eta) + \varepsilon Z_1(\xi, \eta)$$

then from the above construction of these functions, we can find that

$$L_\varepsilon \bar{u}_{\text{as}} \leqslant C\varepsilon \quad \text{and} \quad |\bar{u}_{\text{as}}|_{\partial\Omega} \leqslant C\varepsilon .$$

Consider the barrier function $\phi = C\varepsilon$, we have

$$L_\varepsilon(\phi \pm \bar{u}_{\text{as}}) \geqslant 0 \quad \text{on } \Omega \quad \text{and} \quad (\phi \pm \bar{u}_{\text{as}})|_{\partial\Omega} \geqslant 0 ,$$

from Lemma 2.1.1 and this concludes our proof.

2.3. Finite element method on Shishkin type mesh: Case (I)

To construct a Shishkin type mesh, we assume that positive integers N_x and N_y are divisible by 2, where N_x and N_y denote the number of mesh points in the x- and y-directions, respectively. In the x-direction, we can construct the Shishkin mesh by dividing the interval [0, 1] into the subintervals $[0, \sigma_x]$ and $[\sigma_x, 1]$. Uniform meshes are then used on each subinterval, each with $N_x/2$ points. Here, σ_x is defined by $\sigma_x = \min\{1/2, 2b_1^{-1}\varepsilon \ln N_x\}$. More explicitly, we have

$$0 = x_0 < x_1 < \cdots < x_{i0} < \cdots < x_{Nx} = 1\,,$$

with $i_0 = N_x/2$, $x_{i0} = \sigma_x$, and

$$h_i = 2\sigma_x N_x^{-1}, \quad \text{for } i = 1, \ldots, i_0\,,$$
$$h_i = 2(1-\sigma_x)N_x^{-1}, \quad \text{for } i = i_0 + 1, \ldots, N_x\,,$$

where $h_i = x_i - x_{i-1}$.

In the y-direction, we follow the same way above by dividing the interval [0, 1] into the subintervals $[0, \sigma_y]$ and $[\sigma_y, 1]$. Uniform meshes are then used on each subinterval, each with $N_y/2$ points. Here, σ_y is defined by $\sigma_y = \min\{1/2, 2b_2^{-1}\varepsilon \ln N_y\}$. More explicitly, we have

$$0 = y_0 < y_1 < \cdots < y_{j_0} < \cdots < y_{N_y} = 1\,,$$

with $j_0 = N_y/2$, $y_{j_0} = \sigma_y$, and

$$k_j = 2\sigma_y N_y^{-1}, \quad \text{for } j = 1, \ldots, j_0\,,$$
$$k_j = 2(1-\sigma_y)N_y^{-1}, \quad \text{for } j = j_0 + 1, \ldots, N_y\,,$$

where $k_j = y_j - y_{j-1}$.

We shall assume that $\sigma_x = 2b_1^{-1}\varepsilon \ln N_x \quad \sigma_y = 2b_2^{-1}\varepsilon \ln N_y$. Otherwise,

$$\varepsilon \geqslant \max\left(\frac{b_1}{4 \ln N_x}, \frac{b_2}{4 \ln N_y}\right),$$

in which case ε is not so small allowing this problem to be analyzed in the classical way, which is not of interest here.

Let $I_i = [x_{i-1}, x_i]$, $I = [0, 1]$, $\tilde{I}_i = I_i \times I$, $h = \max_{1 \leqslant i \leqslant N_x} h_i$, $K_j = [y_{j-1}, y_j]$, $\tilde{K}_j = I \times K_j$, $k = \max_{1 \leqslant j \leqslant N_y} k_j$ and $\|\cdot\|_{p,\tau}$ be the L^p norm on any domain τ, here $1 \leqslant p \leqslant \infty$. For simplicity, we use $\|\cdot\|$ to denote the usual L^2 norm on Ω.

The weak formulation of (3) is: find $u \in H_0^1(\Omega)$ such that

$$B(u, v) \equiv (\varepsilon u_x, v_x) + (\varepsilon u_y, v_y) - (b_1 u_x, v) - (b_2 u_y, v) + (au, v) = (f, v), \quad \forall\, v \in H_0^1(\Omega)\,,$$

where $(\cdot,\cdot)$ denotes the usual $L^2(\Omega)$ inner product and $H_0^1(\Omega)$ is the usual Sobolev space [3].

Denote the weighted energy norm by

$$|||v||| \equiv \{\varepsilon\|v_x\|^2 + \varepsilon\|v_y\|^2 + \|v\|^2\}^{1/2}, \ \forall\, v \in H_0^1(\Omega)\,.$$

Note that for any $v \in H_0^1(\Omega)$, we have

$$B(v, v) = (\varepsilon v_x, v_x) + (\varepsilon v_y, v_y) - (b_1 v_x, v) - (b_2 v_y, v) + (av, v)$$
$$= \varepsilon\|v_x\|^2 + \varepsilon\|v_y\|^2 + a\|v\|^2 \geqslant \min(1, a)|||v|||^2\,.$$

Let $S_h(\Omega) \subseteq H_0^1(\Omega)$ be the ordinary bilinear finite element space [3,32] and

$$\Pi w \equiv \sum_{i=0}^{N_x}\sum_{j=0}^{N_y} w_{ij} l_i(x) l_j(y) \tag{5}$$

be the standard bilinear interpolate of w, where Π_x and Π_y are the interpolates in x- and y-directions, respectively. Here, $l_i(x)$ is the well-known 'hat' function [32].

We seek the finite element solution $u^h \in S_h$ such that

$$B(u^h, v) \equiv (\varepsilon u_x^h, v_x) + (\varepsilon u_y^h, v_y) - (b_1 u_x^h, v) - (b_2 u_y^h, v) + (au^h, v) = (\bar{f}, v), \quad \forall v \in S_h, \tag{6}$$

where $\bar{f}$ denotes the standard bilinear interpolate of f.

Let us recall some results from [32] we will use in this paper.

LEMMA 2.3.1 [32, Theorem 2.1] $\Pi w = \Pi_x \Pi_y w = \Pi_y \Pi_x w$.

LEMMA 2.3.2 [32, Theorem 2.6] $\|w - \Pi_x w\|_{\infty,\bar{I}_i} \leq \frac{1}{8} h_i^2 \|w_{xx}\|_{\infty,\bar{I}_i}$.

LEMMA 2.3.3 [32, Lemma 2.1]

$$\|\Pi_x u\|_{\infty,\bar{I}_i} \leq \max_{y \in I}(|u(x_{i-1}, y)|, |u(x_i, y)|),$$

$$\|\Pi_x u\|_{\infty,\Omega} \leq \|u\|_{\infty,\Omega}.$$

The same results of Lemmas 2.3.2 and 2.3.3 hold true for the interpolate Π_y in the y-direction.

2.4. Uniform convergence analysis

In this subsection, we will use the asymptotic expansion given in subsection 2.2 and the technique we used in [21,22] to prove that our FEM is first-order uniformly convergent in L^2 norm.

Let us first prove some interpolation estimates for the solution u of (3), (4).

LEMMA 2.4.1. For the solution u of (3), (4), we have

$$(I) \quad \|u - \Pi_x u\|_{\infty,\bar{I}_i} \leq C(N_x^{-2} \ln^2 N_x + \varepsilon), \quad \forall i = 1, \ldots, i_0, \tag{7}$$

$$(II) \quad \|u - \Pi_y u\|_{\infty,\bar{K}_j} \leq C(N_y^{-2} \ln^2 N_y + \varepsilon), \quad \forall j = 1, \ldots, j_0 \tag{8}$$

$$(I') \quad \|u - \Pi_x u\|_{\infty,\bar{I}_j} \leq C(N_x^{-2} + \varepsilon), \quad \forall i = i_0 + 1, \ldots, N_x, \tag{9}$$

$$(II') \quad \|u - \Pi_y u\|_{\infty,\bar{K}_j} \leq C(N_y^{-2} + \varepsilon), \quad \forall j = j_0 + 1, \ldots, N_y. \tag{10}$$

PROOF. First, for $i = 1, \ldots, i_0$, by Lemmas 2.3.2 and 2.1.6, we obtain

$$\|u - \Pi_x u\|_{\infty,\bar{I}_i} \leq Ch_i^2 \|u_{xx}\|_{\infty,\bar{I}_i} \leq Ch_i^2 \max_{x \in I_i}(1 + \varepsilon^{-2} e^{(-\alpha x)/\varepsilon} + \varepsilon^{-2} e^{(-\alpha(1-x))/\varepsilon})$$

$$\leq Ch_i^2(1 + \varepsilon^{-2}) \leq CN_x^{-2} \ln^2 N_x,$$

since $h_i = 2\sigma_x / N_x$ in this case. Hence, (I) is true.

Second, for $i = i_0 + 1, \ldots, N_x$, in this case $x \in [\sigma_x, 1]$. Use Lemma 2.2.1, we can write $\Pi_x u$ in the form

$$\Pi_x u = \Pi_x U_0 + \Pi_x V_0 + \Pi_x W_0 + \Pi_x Z_0 + \Pi_x R$$

where $\Pi_x U_0$, $\Pi_x V_0$, $\Pi_x W_0$, $\Pi_x Z_0$ and $\Pi_x R$ denote the linear interpolation in the x-direction to U_0, V_0, W_0, Z_0 and R, respectively.

Note that $U_0(x, y)$ is independent of ε, we have

$$\|U_0 - \Pi_x U_0\|_{\infty,\bar{I}_i} \leq Ch_i^2 \|(U_0)_{xx}\|_{\infty,\bar{I}_i} \leq CN_x^{-2},$$

where in the last step we used the fact that $N_x^{-1} \leq h_i \leq 2N_x^{-1}$ for $i = i_0 + 1, \ldots, N_x$.

By Lemma 2.3.3 and the expression of V_0, we have

$$\left\|V_0\left(\frac{x}{\varepsilon}, y\right) - \Pi_x V_0\left(\frac{x}{\varepsilon}, y\right)\right\|_{\infty,\bar{I}_i} \leq 2\left\|V_0\left(\frac{x}{\varepsilon}, y\right)\right\|_{\infty,\bar{I}_i} \leq C\,\mathrm{e}^{(-b_1 x_{i-1})/\varepsilon} \leq C\,\mathrm{e}^{(-b_1\sigma_x)/\varepsilon} = CN_x^{-2},$$

$$\left\|W_0\left(x, \frac{y}{\varepsilon}\right) - \Pi_x W_0\left(x, \frac{y}{\varepsilon}\right)\right\|_{\infty,\bar{I}_i} \leq Ch_i^2\|(W_0)_{xx}\|_{\infty,\bar{I}_i} \leq CN_x^{-2}, \quad \text{since } \mathrm{e}^{-b_2\eta} \leq 1,$$

$$\left\|Z_0\left(\frac{x}{\varepsilon}, \frac{y}{\varepsilon}\right) - \Pi_x Z_0\left(\frac{x}{\varepsilon}, \frac{y}{\varepsilon}\right)\right\|_{\infty,\bar{I}_i} \leq 2\left\|Z_0\left(\frac{x}{\varepsilon}, \frac{y}{\varepsilon}\right)\right\|_{\infty,\bar{I}_i}$$
$$\leq C\,\mathrm{e}^{(-b_1 x_{i-1})/\varepsilon} \leq C\,\mathrm{e}^{(-b_1\sigma_x)/\varepsilon} = CN_x^{-2},$$

and

$$\|R(x, y) - \Pi_x R(x, y)\|_{\infty,\bar{I}_i} \leq 2\|R\|_{\infty,\bar{I}_i} \leq C\varepsilon,$$

which concludes the proof of (I′).

Similarly, we can prove (II) and (II′) in the same way by symmetry consideration.

Then, we have:

LEMMA 2.4.2. For the solution u of (3), (4), we have

(*I*) $\|u - \Pi u\|_{\infty,\Omega} \leq C(N_x^{-2}\ln^2 N_x + N_y^{-2}\ln^2 N_y + \varepsilon)$,

(*II*) $\|u - \Pi u\|_{\infty,[\sigma_x,1]\times[\sigma_y,1]} \leq C(N_x^{-2} + N_y^{-2} + \varepsilon)$.

PROOF. Using Lemmas 2.3.2, 2.3.3 and 2.4.1, we have

$$\|u - \Pi u\|_{\infty,\Omega} \leq \|u - \Pi_x u\|_{\infty,\Omega} + \|\Pi_x(u - \Pi_y u)\|_{\infty,\Omega} \tag{11}$$

$$\leq \|u - \Pi_x u\|_{\infty,\Omega} + \|u - \Pi_y u\|_{\infty,\Omega} \tag{12}$$

$$\leq \max_{1\leq i\leq N_x}\|u - \Pi_x u\|_{\infty,\bar{I}_i} + \max_{1\leq j\leq N_y}\|u - \Pi_y u\|_{\infty,\bar{K}_j}, \tag{13}$$

which concludes our proof.

From now on, we denote $\chi = \Pi u - u^h$ and assume

(A*) $0 < C_1 N_x \leq N_y \leq C_2 N_x$,

(B*) $\varepsilon \leq \max(N_x^{-2}\ln^2 N_x, N_y^{-2}\ln^2 N_y)$,

where (*A**) ensures that we have a quasi-uniform mesh [3, p. 106] away from the boundary layers.

LEMMA 2.4.3. Let $\tau \equiv [0, h_x]\times[0, h_y]$, *then for any* $v \in S_h(\Omega)$ *we have*

(*I*) $\displaystyle\int_\tau |v_x|\,\mathrm{d}x\,\mathrm{d}y \leq C(h_y/h_x)^{1/2}\|v\|_{2,\tau}$,

(*II*) $\displaystyle\int_\tau |v_y|\,\mathrm{d}x\,\mathrm{d}y \leq C(h_x/h_y)^{1/2}\|v\|_{2,\tau}$,

PROOF. (I) This result can be obtained by using the standard homogeneity argument [3]. Let $\bar{\tau} \equiv [0, 1]\times[0, 1]$, so τ can be obtained by the transformation $x = h_x\bar{x}$, $y = h_y\bar{y}$, where $0 \leq \bar{x} \leq 1$, $0 \leq \bar{y} \leq 1$. Hence, we have

$$\int_\tau |v_x|\,\mathrm{d}x\,\mathrm{d}y = \int_{\bar{\tau}} |v_{\bar{x}}|\frac{1}{h_x}h_x h_y\,\mathrm{d}\bar{x}\,\mathrm{d}\bar{y} = h_y\int_{\bar{\tau}} |v_{\bar{x}}|\,\mathrm{d}\bar{x}\,\mathrm{d}\bar{y}$$
$$\leq Ch_y\int_{\bar{\tau}} |v|\,\mathrm{d}\bar{x}\,\mathrm{d}\bar{y} = Ch_y\int_\tau |v|\frac{1}{h_x h_y}\,\mathrm{d}x\,\mathrm{d}y = \frac{C}{h_x}\int_\tau |v|\,\mathrm{d}x\,\mathrm{d}y$$
$$\leq Ch_x^{-1}\|v\|_{2,\tau}(h_x h_y)^{1/2} = C\left(\frac{h_y}{h_x}\right)^{1/2}\|v\|_{2,\tau}$$

which concludes our proof.

(II) The proof is similar to (I).

LEMMA 2.4.4. For the solution u of (3), (4), under the assumptions of (A) and (B*), we have*

(I) $\|(b_1(\Pi u - u)_x, \chi)\| \leq C(N_x^{-1} + N_y^{-1})\|\chi\|$

(II) $\|(b_2(\Pi u - u)_y, \chi)\| \leq C(N_x^{-1} + N_y^{-1})\|\chi\|$

PROOF. (I) Integrating by parts, we have

$$-(b_1(\Pi u - u)_x, \chi) = (b_1(\Pi u - u), \chi_x) = \left(\int_{S_1} + \int_{S_2} + \int_{S_3}\right) b_1(\Pi u - u)\chi_x \, dx\, dy,$$

where $S_1 = [0, 1] \times [0, \sigma_y]$, $S_2 = [0, \sigma_x] \times [\sigma_y, 1]$ and $S_3 = [\sigma_x, 1] \times [\sigma_y, 1]$.

Note that

$$\begin{aligned}\left|\int_{S_1} b_1(\Pi u - u)\chi_x \, dx\, dy\right| &\leq C\|\Pi u - u\|_{\infty, S_1} \int_{S_1} |\chi_x| \, dx\, dy \\ &\leq C(N_x^{-2} \ln^2 N_x + N_y^{-2} \ln^2 N_y + \varepsilon)(\text{Area } S_1)^{1/2}\|\chi_x\| \\ &\leq C(N_x^{-2} \ln^2 N_x + N_y^{-2} \ln^2 N_y + \varepsilon) \ln^{1/2} N_y \|\varepsilon^{1/2}\chi_x\|, \quad \text{since (Area } S_1) \\ &= 2b_2^{-1}\varepsilon \ln N_y .\end{aligned}$$

and

$$\begin{aligned}\left|\int_{S_2} b_1(\Pi u - u)\chi_x \, dx\, dy\right| &\leq C\|\Pi u - u\|_{\infty, S_2} \int_{S_2} |\chi_x| \, dx\, dy \\ &\geqslant C(N_x^{-2} \ln^2 N_x + N_y^{-2} \ln^2 N_y + \varepsilon)(\text{Area } S_2)^{1/2}\|\chi_x\| \\ &\leq C(N_x^{-2} \ln^2 N_x + N_y^{-2} \ln^2 N_y + \varepsilon) \ln^{1/2} N_x \|\varepsilon^{1/2}\chi_x\|, \quad \text{since (Area } S_2) \\ &\leqslant 2b_1^{-1}\varepsilon \ln N_x .\end{aligned}$$

Finally, by Lemmas 2.4.2 and 2.4.3, we have

$$\begin{aligned}\left|\int_{S_3} b_1(\Pi u - u)\chi_x \, dx\, dy\right| &\leq C\|\Pi u - u\|_{\infty, S_3} \int_{S_3} |\chi_x| \, dx\, dy \\ &\leq C(N_x^{-2} + N_y^{-2} + \varepsilon)(h_y/h_x)^{1/2} \sum_{\tau \in S_3} \|\chi\|_{2,\tau} \\ &\leq C(N_x^{-2} + N_y^{-2} + \varepsilon)(h_y/h_x)^{1/2} \left(\sum_{\tau \in S_3} \|\chi\|_{2,\tau}^2\right)^{1/2} \left(\sum_{\tau \in S_3} 1\right)^{1/2} \\ &\leq C(N_x^{-2} + N_y^{-2} + \varepsilon)N_x\|\chi\|_{2,S_3}\end{aligned}$$

where we used the assumption (A*) and the fact that

$$N_x^{-1} \leqslant h_x \leqslant 2N_x^{-1} \quad \text{and} \quad N_y^{-1} \leqslant h_y \leqslant 2N_y^{-1} \quad \text{in } S_3 .$$

From the above inequalities and the assumptions of (A*) and (B*), we conclude our proof of (I). Here, we used the fact that $0 < (\ln^{2.5} N)/N < 0.9$ for $N > 1$, since the maximum value is approximately equal to 0.8045, a value attained for $N = 12.1825$.

(II) The proof is similar to (I).

THEOREM 2.4.1. Let u_h be the finite element solution of (6) and u be the solution of (3), (4). Under the assumption of (A) and (B*), we have*

$$\|u - u^h\| \leqslant C(N_x^{-1} + N_y^{-1}) .$$

PROOF. Note that

$$C_1\|\Pi u - u^h\|^2 \leq B(\Pi u - u^h, \Pi u - u^h) \tag{14}$$

$$= \mathrm{B}(\Pi u - u, \Pi u - u^h) + B(u - u^h, \Pi u - u^h)\,. \tag{15}$$

By the definition of (6), we have

$$B(\Pi u - u, \Pi u - u^h) = \varepsilon((\Pi u - u)_x, \chi_x) + \varepsilon((\Pi\, u - u)_y, \chi_y) - (b \cdot \nabla(\Pi u - u), \chi) + (a(\Pi u - u), \chi)$$

Integrating by parts, we obtain

$$\begin{aligned}
\varepsilon((\Pi u - u)_x, \chi_x) &= \sum_{1\leq i\leq N_x, 1\leq j\leq N_y} \int_{x_{i-1}}^{x_i}\int_{y_{j-1}}^{y_j} \varepsilon(\Pi u - u)_x \chi_x \,\mathrm{d}x\,\mathrm{d}y \\
&= \sum_{1\leq i\leq N_x, 1\leq j\leq N_y} \int_{y_{j-1}}^{y_j} \varepsilon(\Pi u - u)\big|_{x=x_{i-1}}^{x=x_i} \chi_x \,\mathrm{d}y\,, \\
&\leq \sum_{1\leq i\leq N_x, 1\leq j\leq N_y} \int_{y_{j-1}}^{y_j} |\varepsilon^{1/2}\chi_x|\,\mathrm{d}y \cdot \varepsilon^{1/2}\|\Pi u - u\|_{\infty,\Omega} \\
&= \sum_{1\leq i\leq N_x} \int_0^1 |\varepsilon^{1/2}\chi_x|\,\mathrm{d}y \cdot \varepsilon^{1/2}\|\Pi u - u\|_{\infty,\Omega} \\
&= \sum_{1\leq i\leq N_x} \int_0^1\int_0^1 |\varepsilon^{1/2}\chi_x|\,\mathrm{d}y\,\mathrm{d}x \cdot \varepsilon^{1/2}\|\Pi u - u\|_{\infty,\Omega} \\
&= \varepsilon^{1/2}N_x\|\Pi u - u\|_{\infty,\Omega} \cdot \int_0^1\int_0^1 |\varepsilon^{1/2}\chi_x|\,\mathrm{d}y\,\mathrm{d}x\,, \\
&\leq C\varepsilon^{1/2}N_x(N_x^{-2}\ln^2 N_x + N_y^{-2}\ln^2 N_y + \varepsilon)\|\varepsilon^{1/2}\chi_x\|\,,
\end{aligned}$$

where we use the fact that χ_x is independent of x in the above proof.

Similarly, we have

$$\varepsilon((\Pi u - u)_y, \chi_y) \leq C\varepsilon^{1/2}N_y(N_x^{-2}\ln^2 N_x + N_y^{-2}\ln^2 N_y + \varepsilon)\|\varepsilon^{1/2}\chi_y\| \tag{16}$$

Also, note that

$$(a(\Pi u - u), \chi) \leq C\|a\|_{\infty,\Omega}\|\Pi u - u\|\,\|\chi\| \leq C\|\Pi u - u\|_{\infty,\Omega}\|\chi\| \tag{17}$$

$$\leq C(N_x^{-2}\ln^2 N_x + N_y^{-2}\ln^2 N_y + \varepsilon)\|\Pi u - u^h\|\,. \tag{18}$$

By Lemma 2.4.4, we have

$$|(b \cdot \nabla(\Pi u - u), \chi)| \leq C(N_x^{-1} + N_y^{-1})\|\chi\| \tag{19}$$

Hence combining above inequalities with assumptions of (A*) and (B*), we have

$$|B(\Pi u - u, \Pi u - u^h)| \leq C(N_x^{-1} + N_y^{-1})\|\chi\|$$

On the other hand,

$$B(u - u^h, \Pi u - u^h) = (f - \bar{f}, \Pi u - u^h) \tag{20}$$

$$\leq C\|f - \bar{f}\|_{\infty,\Omega}\|\Pi u - u^h\| \leq C(N_x^{-2} + N_y^{-2})\|\Pi u - u^h\|\,. \tag{21}$$

Using (14)–(21), we have

$$\|\Pi u - u^h\| \leq C(N_x^{-1} + N_y^{-1})$$

Therefore using Lemma 2.4.2(I), we obtain

$$\|u - u^h\| \leq \|u - \Pi u\| + \|\Pi u - u^h\| \leq \|u - \Pi u\|_{\infty,\Omega} + \|\!|\Pi u - u^h|\!\| \tag{22}$$

$$\leq C(N_x^{-2} \ln^2 N_x + N_x^{-2} \ln^2 N_y + \varepsilon + N_x^{-1} + N_y^{-1}) . \tag{23}$$

which concludes our proof.

REMARK 2.2. Unlike the reaction-diffusion type problems [22] we usually have only first-order uniform convergence rate in L^2 norm for convection-diffusion type problems. This fact was also observed in one space dimension, cf. Kellogg and Stynes [19] and Roos et al. [30]. Since we cannot use duality techniques [3] to improve error estimates for singularly perturbed problems, which depend on a small parameter ε, we obtained only the above mentioned first order uniform convergence.

2.5. Streamline diffusion finite element methods

In this section, we will present a brief discussion about the popular streamline diffusion method as presented by Johnson et al. [17].

A description of the streamline diffusion finite element method is as follows: Find $u^h \in S_h$ such that

$$B_{SD}(u^h, v) \equiv \varepsilon(\nabla u^h, \nabla v) + (-b \cdot \nabla u^h + a u^h, v - \delta b \cdot \nabla v) = (\bar{f}, v - \delta b \cdot \nabla v), \forall\, v \in S_h ,$$

where $\bar{f}$ denotes the standard bilinear interpolate of f.

Then, it is easy to see that for any $v \in S_h$, we have

$$B_{SD}(v, v) = \varepsilon\|\nabla v\|^2 + \delta\|b \cdot \nabla v\|^2 + a\|v\|^2 \equiv \|\!|v|\!\|_{SD}^2 . \tag{24}$$

Hence

$$\begin{aligned} \|\!|\Pi u - u^h|\!\|_{SD}^2 &\leq B_{SD}(\Pi u - u^h, \Pi u - u^h) \\ &= B_{SD}(\Pi u - u, \chi) + B_{SD}(u - u^h, \chi) \end{aligned}$$

Note that

$$B_{SD}(\Pi u - u, \chi) = B(\Pi u - u, \chi) + (b \cdot \nabla(\Pi u - u), \delta b \cdot \nabla\chi) - (a(\Pi u - u), \delta b \cdot \nabla\chi)$$

and

$$\begin{aligned} B_{SD}(u - u^h, \chi) &= \varepsilon(\nabla u, \nabla\chi) + (-b \cdot \nabla u + au, \chi - \delta b \cdot \nabla\chi) - (\bar{f}, \chi - \delta b \cdot \nabla\chi) \\ &= -\varepsilon(\Delta u, \delta b \cdot \nabla\chi) + (f - \bar{f}, \chi - \delta b \cdot \nabla\chi) \end{aligned}$$

By carrying out a proof similar to that in last section, we can obtain uniform stability for $\|\!|\Pi u - u^h|\!\|_{SD}$ only when $\delta \leq C\varepsilon^n$, where $n > 1$. The different term originates in the perturbation term $\varepsilon(\Delta u, \delta\chi_b)$. Since

$$|\varepsilon(\Delta u, \delta b \cdot \nabla\chi)| \leq \varepsilon\delta\|\Delta u\|\,\|b \cdot \nabla\chi\| \leq C\varepsilon\,\delta\varepsilon^{-3/2}\|b \cdot \nabla\chi\| \leq C\,\delta\epsilon^{-1}\|\varepsilon^{1/2} b \cdot \nabla\chi\| ,$$

we see that only when $\delta \leq C\varepsilon^n$, $n < 1$ can we obtain the uniform stability.

3. Parabolic boundary layer case

In this section, we consider the equation

$$\bar{L}_\varepsilon u \equiv -\varepsilon^2\left(\frac{\partial^2 u}{\partial x^2} + \frac{\partial^2 u}{\partial y^2}\right) + b\frac{\partial u}{\partial y} + a^2 u = f(x, y) \quad \text{in } \Omega \equiv (0, 1) \times (0, 1) \tag{25}$$

$$u = 0 \quad \text{on } \partial\Omega , \tag{26}$$

which corresponds to the case of $\alpha = 2$ in (1). For simplicity, we assume that b and a are positive constants. It is easy to see that $\bar{L}_\varepsilon$ satisfy the same weak maximum principle. This problem is different from the last one in

Section 2 in that it has complicated parabolic boundary layers [5,8,34,35,36] at $x = 0$ and $x = 1$ except for the ordinary exponential boundary layer at $y = 1$.

3.1. Derivative estimates of the solution

In this subsection, we will obtain some derivative estimates for the solution u of (25), (26) under compatibility conditions H^*. Since the proofs are very similar to those in the last problem, we will just sketch the important steps.

LEMMA 3.1.1.

(*I*) $|u(x, y)| \leq C(1 - e^{(-2b(1-y))/\varepsilon^2})$ on $\bar{\Omega}$,
(*II*) $|u(x, y)| \leq Cy$ on $\bar{\Omega}$,
(*III*) $|u(x, y)| \leq C(1 - e^{(-ax)/\varepsilon})$ on $\bar{\Omega}$,
(*IV*) $|u(x, y)| \leq C(1 - e^{(-a(1-x))/\varepsilon})$ on $\bar{\Omega}$.

PROOF. (I) Use the barrier function $\phi(x, y) = C(1 - e^{(-2b(1-y))/\varepsilon^2})$.
(II) Use the barrier function $\phi(x, y) = Cy$.
(III) Use the barrier function $\phi(x, y) = C(1 - e^{-ax/\varepsilon})$.
(IV) Use the barrier function $\phi(x, y) = C(1 - e^{-a(1-x)/\varepsilon})$.

LEMMA 3.1.2

(*I*) $|u_y(x, y)| \leq C\varepsilon^{-2}$ on $\partial\Omega$,
(*II*) $|u_x(x, y)| \leq C\varepsilon^{-1}$ on $\partial\Omega$.

PROOF. (I) By Lemma 3.1.1(I), we have

$$|u_y(x, 1)| = \left| \lim_{y \to 1^-} \frac{u(x, 1) - u(x, y)}{(1 - y)} \right| \leq \lim_{y \to 1^-} \left| \frac{u(x, 1) - u(x, y)}{(1 - y)} \right|$$

$$\leq \lim_{y \to 1^-} \frac{C(1 - e^{(-2b(1-y))/\varepsilon^2})}{(1 - y)} = \frac{2bC}{\varepsilon^2}.$$

The rest of the proof is similar to Lemma 2.1.2.

LEMMA 3.1.3.

(*I*) $|u_y(x, y)| \leq C(1 + \varepsilon^{-2} e^{(-b(1-y))/\varepsilon^2})$ on $\bar{\Omega}$,
(*II*) $|u_x(x, y)| \leq C(1 + \varepsilon^{-1} e^{(-ax)/\varepsilon} + \varepsilon^{-1} e^{(-a(1-x))/\varepsilon})$ on $\bar{\Omega}$.

PROOF. (*I*) Consider the barrier function $\phi(x, y) = C(1 + \varepsilon^{-2} e^{(-b(1-y))/\varepsilon^2})$.
(II) Consider the barrier function $\phi(x, y) = C(1 + \varepsilon^{-1} e^{(-ax)/\varepsilon} + \varepsilon^{-1} e^{(-a(1-x))/\varepsilon})$.

LEMMA 3.1.4.

(*I*) $|u_{yy}(x, y)| \leq C\varepsilon^{-4}$ on $\partial\Omega$
(*II*) $|u_{xx}(x, y)| \leq C\varepsilon^{-2}$ on $\partial\Omega$.

PROOF. (I) Using the given boundary conditions (26), we have $u_{yy}|_{x=0,1} = 0$. From Eq. (25), we have $u_{yy}|_{y=0,1} = (b\,\partial u/\partial y - f)/\varepsilon^2|_{y=0,1} \leq C\varepsilon^{-4}$.
(II) Using the given boundary conditions, we obtain $u_{xx}|_{y=0,1} = 0$. From Eq. (25), we have

$$u_{xx}|_{x=0,1} = f/\varepsilon^2|_{x=0,1} \leq C\varepsilon^{-2}.$$

LEMMA 3.1.5.

(*I*) $|u_{yy}(x, y)| \leq C(1 + \varepsilon^{-4} e^{(-b(1-y))/\varepsilon^2})$ *on* $\overline{\Omega}$,

(*II*) $|u_{xx}(x, y)| \leq C(1 + \varepsilon^{-2} e^{(-ax)/\varepsilon} + \varepsilon^{-2} e^{(-a(1-x))/\varepsilon})$ *on* $\overline{\Omega}$.

PROOF. (I) Use the barrier function $\phi(x, y) = C(1 + \varepsilon^{-4} e^{(-b(1-y))/\varepsilon^2})$.

(II) Use the barrier function $\phi(x, y) = C(1 + \varepsilon^{-2} e^{(-ax)/\varepsilon} + \varepsilon^{-2} e^{(-a(1-x))/\varepsilon})$.

3.2. The asymptotic expansion

This subsection is based on the work of Butuzov [5]. Here, we will use the zero order of Butuzov asymptotic expansion [5, p. 781, (5)]:

$$u_{as} = u_0(x, y) + Q_0^{(1)}(\xi_1, y) + Q_0^{(2)}(\xi_2, y) + V_0(x, \eta) + P_0^{(1)}(\xi_1, \eta) + P_0^{(2)}(\xi_2, \eta) + R_0^{(1)}(\zeta_1, \eta) + R_0^{(2)}(\zeta_2, \eta),$$

where

$$\xi_1 = \frac{x}{\varepsilon}, \qquad \xi_2 = \frac{1-x}{\varepsilon}, \qquad \eta = \frac{1-y}{\varepsilon^2}, \qquad \zeta_1 = \frac{x}{\varepsilon^2} \quad \text{and} \quad \zeta_2 = \frac{1-x}{\varepsilon^2}.$$

LEMMA 3.2.1. Assume $f(0, 0) = f(1, 0) = 0$, *then for sufficiently small* ε, *we have*

$$|\Delta(x, y)| \leq C\varepsilon, \quad \forall (x, y) \in \overline{\Omega},$$

where $\Delta(x, y) = u(x, y) - u_{as}(x, y)$ *is the remainder of the above asymptotic expansion.*

The above result corresponds to the case $n = 0$ in 5, [p. 787, Theorem]. In the following we will present additional details for each term.

The regular part u_0 satisfies the following equation [5, p. 781, (6)]:

$$b\frac{\partial u_0}{\partial y} + a^2 u_0 = f, \quad \text{in } \Omega,$$

$$u_0(x, 0) = 0$$

The parabolic layer function $Q_0^{(1)}(\xi_1, y)$ [5, p. 782] at $x = 0$ satisfies

$$\frac{\partial^2 Q_0^{(1)}}{\partial \xi_1^2} - b\frac{\partial Q_0^{(1)}}{\partial y} - a^2 Q_0^{(1)} = 0,$$

$$Q_0^{(1)}(0, y) = -u_0(0, y), \qquad Q_0^{(1)}(\xi_1, 0) = 0,$$

$$Q_0^{(1)}(\xi_1, y) \to 0 \qquad \text{as } \xi_1 \to \infty$$

Also, we have the following estimates [5, p. 783]:

$$\left| \frac{\partial^{2m} Q_0^{(1)}(\xi_1, y)}{\partial \xi_1^{2m}} \right| \leq C e^{-\alpha \xi_1}, \quad \text{for } \xi_1 \geq 0, 0 \leq y \leq 1, \quad m = 0, 1.$$

$$\left| \frac{\partial^{m} Q_0^{(1)}(\xi_1, y)}{\partial y^{m}} \right| \leq C e^{-\alpha \xi_1}, \quad \text{for } \xi_1 \geq 0, 0 \leq y \leq 1, \quad m = 0, 1, 2.$$

For the parabolic layer function $Q_0^{(2)}(\xi_2, y)$ at $x = 1$ we have the similar estimates as $Q_0^{(1)}(\xi_1, y)$.

To eliminate the discrepancies introduced by $u_0(x, y)$, $Q_0^{(1)}(\xi_1, y)$ and $Q_0^{(2)}(\xi_2, y)$ at $y = 1$, we need to define functions $V_0(x, \eta)$, $P_0^{(1)}(\xi_1, \eta)$ and $P_0^{(2)}(\xi_2, \eta)$ as follows:

The function $V_0(x, \eta)$ satisfies the following equation:

$$\frac{\partial^2 V_0}{\partial \eta^2} + b\frac{\partial V_0}{\partial \eta} = 0, \quad \text{for } \eta > 0$$

$$V_0(x, 0) = -u_0(x, 1)$$

From which we obtain its solution as $V_0(x,\eta) = -u_0(x,1)\,e^{-b\eta}$. Hence, we have

$$|V_0(x,\eta)| \leq C\,e^{-\alpha\eta}, \quad \text{for } \eta \geq 0$$

The function $P_0^{(1)}(\xi_1,\eta)$ satisfies the following equation:

$$\frac{\partial^2 P_0^{(1)}}{\partial \eta^2} + b\frac{\partial P_0^{(1)}}{\partial \eta} = 0, \quad \text{for } \eta > 0$$

$$P_0^{(1)}(\xi_1,0) = -Q_0^{(1)}(\xi_1,1)$$

$$P_0^{(1)}(\xi_1,\eta) \to 0, \quad \text{when } \eta \to \infty$$

From which we obtain its solution as $P_0^{(1)}(\xi_1,\eta) = -Q_0^{(1)}(\xi_1,1)\,e^{-b\eta}$. Hence

$$|P_0^{(1)}(\xi_1,\eta)| \leq C\,e^{-\alpha(\xi_1+\eta)}, \quad \text{for } \xi_1 \geq 0, \eta \geq 0.$$

Similarly, we can find that $P_0^{(2)}(\xi_2,\eta) = -Q_0^{(2)}(\xi_2,1)\,e^{-b\eta}$.

To eliminate the discrepancies introduced by functions $V_0(x,\eta) + P_0^{(1)}(\xi_1,\eta)$ and $V_0(x,\eta) + P_0^{(2)}(\xi_2,\eta)$ at the corners (0, 1) and (1, 1), we use the functions $R_0^{(1)}(\zeta_1,\eta)$ and $R_0^{(2)}(\zeta_2,\eta)$.

Function $R_0^{(1)}(\zeta_1,\eta)$ satisfies the following equation [5, p. 786]:

$$\frac{\partial^2 R_0^{(1)}}{\partial \zeta_1^2} + \frac{\partial^2 R_0^{(1)}}{\partial \eta^2} + b\frac{\partial R_0^{(1)}}{\partial \eta} = 0 \quad \text{for } \zeta_1 > 0, \eta > 0$$

$$R_0^{(1)}(\zeta_1,0) = 0, \qquad R_0^{(1)}(0,\eta) = -(V_0^{(1)}(0,\eta) + P_0^{(1)}(0,\eta))$$

$$R_0^{(1)}(\zeta_1,\eta) \to 0, \quad \text{when } \sqrt{\zeta_1^2+\eta^2} \to \infty$$

Its solution is given by [5, p. 786, (35)]:

$$R_0^{(1)}(\zeta_1,\eta) = \tilde{R}(\xi,\eta)\,e^{-b\eta/2} + (V_0^{(1)}(0,\eta) + P_0^{(1)})(0,\eta))\,e^{-b\zeta_1/2},$$

where [5, p. 787, (41)]

$$|\tilde{R}(\zeta_1,\eta)| \leq C\,e^{-\alpha\sqrt{\zeta_1^2+\eta^2}}$$

From which we obtain

$$|R_0^{(1)}(\zeta_1,\eta)| \leq C\,e^{-\alpha(\zeta_1+\eta)}$$

Similar results hold true for $R_0^{(2)}(\zeta_2,\eta)$.

3.3. Finite element method on Shishkin type mesh: Case (II)

To construct a Shishkin type mesh, we assume that the positive integer N_x is divisible by 4 while N_y is divisible by 2, where N_x and N_y denote the number of mesh points in the x- and y-directions, respectively. In x-direction, we can construct the Shishkin mesh by dividing the interval [0, 1] into the subintervals $[0,\sigma_x]$, $[\sigma_x, 1-\sigma_x]$ and $[1-\sigma_x, 1]$. Uniform meshes are then used on each subinterval, with $N_x/4$ points on each of $[0,\sigma_x]$ and $[1-\sigma_x, 1]$ and $N_x/2$ points on $[\sigma_x, 1-\sigma_x]$. Here σ_x is defined by $\sigma_x = \min\{1/4, 2a^{-1}\varepsilon \ln N_x\}$. More explicitly, we have

$$0 = x_0 < x_1 < \cdots < x_{i_0} < \cdots < x_{N_x - i_0} \cdots < x_{N_x} = 1,$$

with $i_0 = N_x/4$, $x_{i_0} = \sigma_x$, $x_{N_x - i_0} = 1 - \sigma_x$, and

$$h_i = 4\sigma_x N_x^{-1}, \quad \text{for } i = 1, \ldots, i_0, N_x - i_0 + 1, \ldots, N_x,$$

$$h_i = 2(1-2\sigma_x)N_x^{-1}, \quad \text{for } i = i_0 + 1, \ldots, N_x - i_0,$$

where $h_i = x_i - x_{i-1}$.

In the y-direction, we follow a similar procedure to that outlined above by dividing the interval [0, 1] into the subintervals $[0, 1-\sigma_y]$ and $[1-\sigma_y, 1]$. Uniform meshes are then used on each subinterval, each with $N_y/2$ points. Here, σ_y is defined by $\sigma_y = \min\{1/2, 2b^{-1}\varepsilon^2 \ln N_y\}$. More explicitly, we have

$$0 = y_0 < y_1 < \cdots < y_{j_0} < \cdots < y_{N_y} = 1\,,$$

with $j_0 = N_y/2$, $y_{j_0} = 1-\sigma_y$, and

$$\mathrm{k_j} = 2(1-\sigma_y)N_y^{-1}, \quad \text{for } j = 1, \ldots, j_0,$$

$$k_j = 2\sigma_y N_y^{-1}, \quad \text{for } j = j_0+1, \ldots, N_y\,,$$

where $k_j = y_j - y_{j-1}$.

We shall assume that $\sigma_x = 2a^{-1}\varepsilon \ln N_x$, $\sigma_y = 2b^{-1}\varepsilon^2 \ln N_y$. In the following we will use the same notations as last section.

The weak formulation of (25) is: find $u \in H_0^1(\Omega)$ such that

$$\bar{B}(u, v) \equiv (\varepsilon^2 u_x, v_x) + (\varepsilon^2 u_y, v_y) + (bu_y, v) + (a^2 u, v) = (f, v), \quad \forall\, v \in H_0^1(\Omega)\,. \tag{27}$$

We seek the finite element solution $u^h \in S_h$ such that

$$\bar{B}(u^h, v) \equiv (\varepsilon^2 u_x^h, v_x) + (\varepsilon^2 u_y^h, v_y) + (bu_y^h, v) + (a^2 u^h, v) = (\bar{f}, v)\,, \quad \forall\, v \in H_0^1(\Omega)\,, \tag{28}$$

where $\bar{f}$ denotes the standard bilinear interpolate of f.

In this section we use the following weighted energy norm

$$|\!|\!| v |\!|\!|_* \equiv \{\varepsilon^2 \|v_x\|^2 + \varepsilon^2 \|v_y\|^2 + \|v\|^2\}^{1/2}\,, \quad \forall\, v \in H_0^1(\Omega)\,.$$

Note that

$$\begin{aligned}\bar{B}(v, v) &= \varepsilon^2 \|v_x\|^2 + \varepsilon^2 \|v_y\|^2 + \left(b\frac{\partial v}{\partial y}, v\right) + (a^2 v, v)\\ &\geqslant \min(1, a^2)(\varepsilon^2 \|v_x\|^2 + \varepsilon^2 \|v_y\|^2 + \|v\|^2)\\ &= \min(1, a^2)|\!|\!| v |\!|\!|_*^2\end{aligned}$$

3.4. Uniform convergence analysis

In this section, we will prove the almost second-order uniform convergence rate in L^2 norm for the problem (25), (26). The proofs are similar to those presented for the last problem. Hence, we just provide some important steps.

LEMMA 3.4.1. For the solution u of (25), (26), we have

(*I*) $\|u - \Pi_x u\|_{\infty, \tilde{I}_i} \leqslant C(N_x^{-2} \ln^2 N_x + \varepsilon)\,, \quad \forall\, i = 1, \ldots, i_0, N_x - i_0 + 1, \ldots, N_x$

(*I'*) $\|u - \Pi_x u\|_{\infty, \tilde{I}_i} \leqslant C(N_x^{-2} + \varepsilon)\,, \quad \forall\, i = i_0 + 1, \ldots, N_x - i_0\,,$

(*II*) $\|u - \Pi_y u\|_{\infty, \tilde{K}_j} \leqslant C(N_y^{-2} \ln^2 N_y + \varepsilon)\,, \quad \forall\, j = j_0 + 1, \ldots, N_y\,,$

(*II'*) $|u - \Pi_y u\|_{\infty, \tilde{K}_j} \leqslant C(N_y^{-2} + \varepsilon)\,, \quad \forall\, j = 1, \ldots, j_0\,.$

PROOF. The proof is similar to Lemma 2.4.1 except that here we will use the asymptotic expansion and the estimates in Subsection 3.2.

By carrying out the similar proof of Lemma 2.4.2, we obtain

LEMMA 3.4.2. For the solution u of (25), (26), we have

(*I*) $\|u - \Pi u\|_{\infty, \Omega} \leqslant C(N_x^{-2} \ln^2 N_x + N_y^{-2} \ln^2 N_y + \varepsilon)$,

(*II*) $\|u - \Pi u\|_{\infty, [\sigma_x, 1-\sigma_x] \times [0, 1-\sigma_y]} \leqslant C(N_x^{-2} + N_y^{-2} + \varepsilon)$.

LEMMA 3.4.3. For the solution u of (25), (26), under the assumptions of (A) and (B*), we have*

$$\|(b(\Pi u - u)_y, \chi)\| \leq C(N_x^{-1} + N_y^{-1})\|\chi\|_* .$$

PROOF. Carrying out an integration by parts,

$$(b(\Pi u - u)_y, \chi) = -(b(\Pi u - u), \chi_y)$$
$$= -\left(\int_{S_1} + \int_{S_2} + \int_{S_3} + \int_{S_4}\right) b(\Pi u - u)\chi_y \, dx \, dy ,$$

where $S_1 = [0, \sigma_x] \times [0, 1 - \sigma_y]$, $S_2 = [\sigma_x, 1 - \sigma_x] \times [0, 1 - \sigma_y]$, $S_3 = [1 - \sigma_x, 1] \times [0, 1 - \sigma_y]$ and $S_4 = [0, 1] \times [1 - \sigma_y, 1]$.

Note that by Lemma 2.4.3, we have

$$\left| \int_{S_1} b(\Pi u - u)\chi_y \, dx \, dy \right| \leq C\|\Pi u - u\|_{\infty, S_1} \int_{S_1} |\chi_y| \, dx \, dy$$
$$\leq C\|\Pi u - u\|_{\infty, S_1} (h_x / h_y)^{1/2} \sum_{\tau \in S_1} \|\chi\|_{2,\tau}$$
$$\leq C\|\Pi u - u\|_{\infty, S_1} (h_x / h_y)^{1/2} \left(\sum_{\tau \in S_1} \|\chi\|_{2,\tau}^2 \right)^{1/2} \left(\sum_{\tau \in S_1} 1 \right)^{1/2}$$
$$\leq C\|\Pi u - u\|_{\infty, S_1} (h_x / h_y)^{1/2} (N_x N_y)^{1/2} \|\chi\|_{2, S_1}$$
$$\leq C(N_x^{-2} \ln^2 N_x + N_y^{-2} \ln^2 N_y + \varepsilon) \varepsilon^{1/2} N_y \ln^{1/2} N_x \|\chi\|_{2, S_1} ,$$

where in the last step, we used Lemma 3.4.2 and the fact that

$$h_x = 2a^{-1} \varepsilon N_x^{-1} \ln N_x \quad \text{and} \quad N_y^{-1} \leq h_y \leq 2N_y^{-1} \quad \text{in } S_1 .$$

Similarly, we have

$$\left| \int_{S_3} b(\Pi u - u)\chi_y \, dx \, dy \right| \leq C(N_x^{-2} \ln^2 N_x + N_y^{-2} \ln^2 N_y + \varepsilon) \varepsilon^{1/2} N_y \ln^{1/2} N_x \|\chi\|_{2, S_3}$$

and by Lemma 2.4.3, we have

$$\left| \int_{S_2} b(\Pi u - u)\chi_y \, dx \, dy \right| \leq C\|\Pi u - u\|_{\infty, S_2} \int_{S_2} |\chi_y| \, dx \, dy$$
$$\leq C\|\Pi u - u\|_{\infty, S_2} (h_x / h_y)^{1/2} \sum_{\tau \in S_2} \|\chi\|_{2,\tau}$$
$$\leq C\|\Pi u - u\|_{\infty, S_2} (h_x / h_y)^{1/2} \left(\sum_{\tau \in S_2} \|\chi\|_{2,\tau}^2 \right)^{1/2} \left(\sum_{\tau \in S_2} 1 \right)^{1/2}$$
$$\leq C\|\Pi u - u\|_{\infty, S_2} (N_y / N_x)^{1/2} (N_x N_y)^{1/2} \|\chi\|_{2, S_2}$$
$$\leq C(N_x^{-2} + N_y^{-2} + \varepsilon) N_y \|\chi\|_{2, S_2}$$

where we used the fact that

$$N_x^{-1} \leq h_x \leq 2N_x^{-1} \quad \text{and} \quad N_y^{-1} \leq h_y \leq 2N_y^{-1} \quad \text{in } S_2 .$$

Finally,

$$\left| \int_{S_4} b(\Pi u - u)\chi_y \, dx \, dy \right| \leq C\|\Pi u - u\|_{\infty, S_4} \int_{S_4} |\chi_y| \, dx \, dy$$
$$\leq C(N_x^{-2} \ln^2 N_x + N_y^{-2} \ln^2 N_y + \varepsilon)(\text{Area } S_4)^{1/2} \|\chi_y\|_{2, S_4}$$
$$\leq C(N_x^{-2} \ln^2 N_x + N_y^{-2} \ln^2 N_y + \varepsilon) \ln^{1/2} N_y \|\varepsilon \chi_y\|_{2, S_4} .$$

From above inequalities and the assumptions of (A*) and (B*), we conclude our proof. Here, we used the fact that $0 > (\ln^{2.5} N)/N < 0.9$ for $N > 1$, since the maximum value is approximately equal to 0.8045, which is achieved at $N = 12.1825$.

THEOREM 3.4.1. Let u_h be the finite element solution of (28) and u be the solution of (25), (26). Then, under the assumptions of (A) and (B*), we have*

$$\|u - u^h\| \leq C(N_x^{-1} + N_y^{-1}) .$$

PROOF. Note that

$$C_1 \|\Pi u - u^h\|_*^2 \leq \bar{B}(\Pi u - u^h, \Pi u - u^h) \tag{29}$$

$$= \bar{B}(\Pi u - u, \Pi u - u^h) + \bar{B}(u - u^h, \Pi u - u^h). \tag{30}$$

From (28) we have

$$\bar{B}(\Pi u - u, \Pi u - u^h) = \varepsilon^2((\Pi u - u)_x, \chi_x) + \varepsilon^2((\Pi u - u)_y, \chi_y) + (b(\Pi u - u)_y, \chi) + (a^2(\Pi u - u), \chi)$$

Integrating by parts, we obtain

$$\begin{aligned}
\varepsilon^2((\Pi u - u)_x, \chi_x) &= \sum_{1 \leq i \leq N_x, 1 \leq j \leq N_y} \int_{x_{i-1}}^{x_i} \int_{y_{j-1}}^{y_j} \varepsilon^2 (\Pi u - u)_x \chi_x \, dx \, dy \\
&= \sum_{1 \leq i \leq N_x, 1 \leq j \leq N_y} \int_{y_{j-1}}^{y_j} \varepsilon^2 (\Pi u - u)|_{x=x_{i-1}}^{x=x_i} \chi_x \, dy , \\
&\leq \sum_{1 \leq i \leq N_x, 1 \leq j \leq N_y} \int_{y_{j-1}}^{y_j} |\varepsilon \chi_x| \, dy \cdot \varepsilon \|\Pi u - u\|_{\infty,\Omega} \\
&= \sum_{1 \leq i \leq N_x} \int_0^1 |\varepsilon \chi_x| \, dy \cdot \varepsilon \|\Pi u - u\|_{\infty,\Omega} \\
&= \sum_{1 \leq i \leq N_x} \int_0^1 \int_0^1 |\varepsilon \chi_x| \, dy \, dx \cdot \varepsilon \|\Pi u - u\|_{\infty,\Omega} , \\
&= \varepsilon N_x \|\Pi u - u\|_{\infty,\Omega} \cdot \int_0^1 \int_0^1 (\tau \varepsilon \chi_x| \, dy \, dx , \\
&\leq C \varepsilon N_x (N_x^{-2} \ln^2 N_x + N_y^{-2} \ln^2 N_y + \varepsilon) \|\varepsilon \chi_x\| ,
\end{aligned}$$

where we use the fact that χ_x is independent of x in the above proof.

Similarly, we have

$$\varepsilon^2((\Pi u - u)_y, \chi_y) \leq C \varepsilon N_y (N_x^{-2} \ln^2 N_x + N_y^{-2} \ln^2 N_y + \varepsilon) \|\varepsilon \chi_y|$$

Also, note that

$$(a^2(\Pi u - u), \chi) \leq C \|a^2\|_{\infty,\Omega} \|\Pi u - u\| \, \|\chi -\| \leq C \|\Pi u - u\|_{\infty,\Omega} \|\chi\| \tag{31}$$

$$C(N_x^{-2} \ln^2 N_x + N_y^{-2} \ln^2 N_y + \varepsilon) \|\Pi u - u^h\| , \tag{32}$$

Combining with Lemma 3.4.3, we have

$$\bar{B}(\Pi u - u, \Pi u - u^h)| \leq C(N_x^{-1} + N_y^{-1}) .$$

On the other hand,

$$\bar{B}(u - u^h, \Pi u - u^h) = (f - \bar{f}, \Pi u - u^h) \tag{33}$$

$$\leq C \|f - \bar{f}\|_{\infty,\Omega} \|\Pi u - u^h\| \leq C(N_x^{-2} + N_y^{-2}) . \tag{34}$$

Combining (31)–(36), we have

$$\|\!|\Pi u - u^h|\!\| \leq C(N_x^{-1} + N_y^{-1}) .$$

Therefore, combining this with Lemma 3.4.2, we obtain

$$\begin{aligned}\|u - u^h\| &\leq \|u - \Pi u\| + \|\Pi u - u^h\| \leq \|u - \Pi u\|_{\infty,\Omega} + \|\!|\Pi u - u^h|\!\| \\ &\leq C(N_x^{-1} + N_y^{-1})\end{aligned}$$

which concludes our proof.

Streamline diffusion finite element methods

For problem (25), (26), Zhou and Rannacher [39] discussed the local super convergence property of the streamline diffusion method. Here will show that the streamline diffusion finite element method will have the same uniform stability as the standard FEM on our Shishkin type mesh.

The streamline diffusion finite element method: Find $u^h \in S_h$ such that

$$\bar{B}_{\mathrm{SD}}(u^h, v) \equiv \varepsilon^2(\nabla u_x^h, \nabla v) + (bu_y^h, v + \delta b v_y) + (a^2 u^h, v + \delta b v_y) = (\bar{f}, v + \delta b\, v_y), \quad \forall\, v \in S_h ,$$

where $\bar{f}$ denotes the standard bilinear interpolate of f.

Then, it is easy to see that: for any $v \in S_h$, we have

$$\bar{B}_{\mathrm{SD}}(v, v) = \varepsilon^2\|\nabla v\|^2 + b\delta\|v_y\|^2 + a^2\|v\|^2 \equiv |\!|\!| v |\!|\!|_{\mathrm{SD}^*}^2 .$$

Hence

$$\begin{aligned}|\!|\!|\Pi u - u^h|\!|\!|_{SD^*}^2 &\leq \bar{B}_{\mathrm{SD}}(\Pi u - u^h, \Pi u - u^h) \\ &= \bar{B}_{\mathrm{SD}}(\Pi u - u, \chi) + \bar{B}_{\mathrm{SD}}(u - u^h, \chi)\end{aligned}$$

Note that

$$\bar{B}_{\mathrm{SD}}(\Pi u - u, \chi) = \bar{B}(\Pi u - u, \chi) + (b(\Pi u - u)_y, \delta b\chi_y) + (a^2(\Pi u - u), \delta b\chi_y)$$

and

$$\begin{aligned}\bar{B}_{\mathrm{SD}}(u - u^h, \chi) &= \bar{B}_{\mathrm{SD}}(u, \chi) - \bar{B}_{\mathrm{SD}}(u^h, \chi) \\ &= \varepsilon^2(\Delta u, \delta b\chi_y) + (f - \bar{f}, \chi + \delta b\chi_y)\end{aligned}$$

By carrying out a proof similar to the one in the last section, we can obtain uniform stability for $|\!|\!|\Pi u - u^h|\!|\!|_{\mathrm{SD}^*}$ only when $\delta \leq C\varepsilon^n$, where $n > 2$. The problem originates from the perturbation term $\varepsilon^2(\Delta u, \delta b\chi_y)$. Since

$$|\varepsilon^2(\Delta u, \delta b\chi_y)| \leq C\varepsilon^2\, \delta |\Delta u| \|\chi_y\| \leq C\varepsilon^2\, \delta\varepsilon^{-3}\|\chi_y\| \leq C\, \delta\varepsilon^{-2}\|\varepsilon\chi_y\| ,$$

we see that only when $\delta \leq C\varepsilon^n$, $n > 2$ can we obtain the uniform stability, where in the second inequality we used the result of Lemma 3.1.5.

4. Numerical experiments

In this section, we will illustrate our methods with two numerical examples. The first one has only typical exponential boundary layers, while the second one has both exponential boundary layers and parabolic boundary layers.

Our computations were carried out in double precision on the IBM SP2 clusters at SCRI. The figures were obtained by MATLAB, where we use (a) to indicate the left figure and (b) to indicate the right figure in each group, respectively. Since our problems are nonsymmetric and very ill-conditioned, we use a preconditioned ILUT-GMRES solver from SPARSKIT provided by Saad [31].

4.1. Example 1

The first example we tested corresponds to the problem given by Eqs. (3), (4) where $b_1 = b_2 = 1$, $a = 2$ and f is chosen appropriately such that the exact solution is

$$u(x, y) = (1 - e^{-x/\varepsilon})(1 - e^{-y/\varepsilon})(1 - x)(1 - y).$$

We see that this solution has typical exponential boundary layers at $x = 0$ and $y = 0$. We choose a bilinear interpolate Πf of f as $\bar{f}$ and $N_x = N_y = N$. The numerical results of our experiments are presented for values of ε ranging from 10^{-8} to 10^{-2} and for mesh resolutions of $N = 12$, 24 and 48, respectively.

First we tested our standard FEM on Shishkin mesh. The computed L^2 error is provided in Table 1. To see more accurately the convergence order, we provide the computed convergence rate

$$R_\varepsilon^N = (\ln e_\varepsilon^N - \ln e_\varepsilon^{2N})/\ln 2$$

in Table 2. Here, e_ε^N is the L^2 error between the exact solution $u(x, y)$ and the computed solution $u^h(x, y)$, where $h = 1/N$. From Table 2, we see that $u^h(x, y)$ approximates $u(x, y)$ uniformly to almost second-order in L^2 norm, which is better than predicted by our theoretical analysis. The condition numbers for the coefficient matrices resulting from the FEM discretization of this problem are provided in Table 3. Here, we calculated the condition number by MATLAB. Using an inverse estimate [3], we can easily see that the condition number $K(A)$ of the coefficient matrix A for this FEM is bounded by $O(\varepsilon N^2 \ln^{-2} N)$, which is also shown by Roos [28]. From Table 3, we see our numerical results are very consistent with the theoretical condition number. The pointwise errors $u_h - u$ are plotted in Figs. 1–6 for different ε and N. The results obtained show very clearly the uniform convergence. They also show that the larger error originates from boundary layers, where in our case the boundary layers are located at $x = 0$ and $y = 0$. The error also displays some oscillations and they pollute other parts of the domain starting from the corner and boundary layers, which is normal for the standard FEM for such convection–diffusion type problems [6,17,38]. To compare our standard FEM with the classical standard FEM on uniform mesh, we performed same computations for the standard FEM on uniform mesh, and we present the

Table 1
Errors in L^2 norm for Example 1

ε	N		
	12	24	48
1.0D − 02	3.9353295D − 03	9.5865477D − 04	3.1808308D − 04
1.0D − 03	5.9899591D − 03	1.4755047D − 03	2.8507499D − 04
1.0D − 04	6.3435845D − 03	1.7507047D − 03	4.3802338D − 04
1.0D − 05	6.3808889D − 03	1.7849438D − 03	4.6954562D − 04
1.0D − 06	6.3848394D − 03	1.7884465D − 03	4.7321017D − 04
1.0D − 07	6.3851212D − 03	1.7887975D − 03	4.7356168D − 04
1.0D − 08	6.3851677D − 03	1.7888327D − 03	4.7359686D − 04

Table 2
Convergence rates R_ε^N in L^2 norm for Example 1

ε	N	
	12	24
1.0D − 02	2.0374	1.5916
1.0D − 03	2.0213	2.3718
1.0D − 04	1.8574	1.9989
1.0D − 05	1.8379	1.9265
1.0D − 06	1.8359	1.9182
1.0D − 07	1.8357	1.9174
1.0D − 08	1.8357	1.9173

Table 3
Condition numbers for Example 1

ε	N	
	12	24
$1.0D-02$	131.7961	393.1111
$1.0D-03$	$1.2027e+03$	$3.4905e+03$
$1.0D-04$	$1.1963e+04$	$3.4211e+04$
$1.0D-05$	$1.1958e+05$	$3.4154e+05$
$1.0D-06$	$1.1958e+06$	$3.4148e+06$
$1.0D-07$	$1.1958e+07$	$3.4147e+07$
$1.0D-08$	$1.1958e+08$	$3.4147e+08$

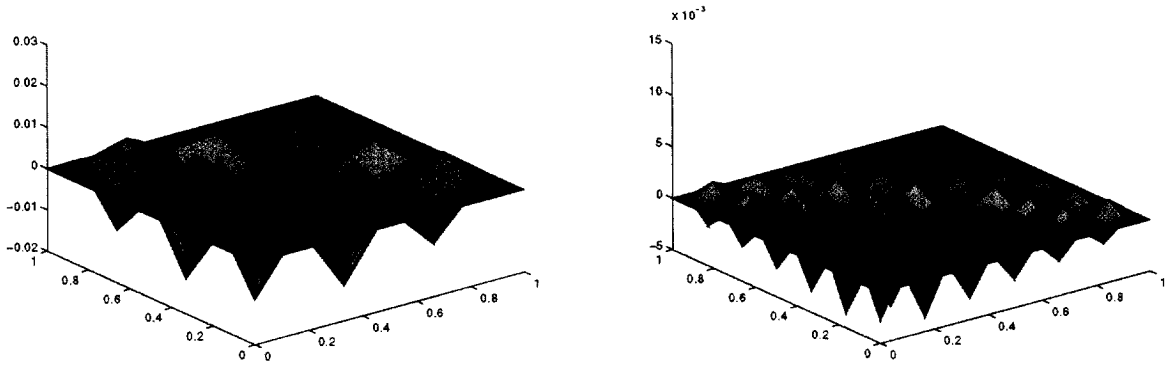

Fig. 1. Example 1: Standard FEM on Shishkin mesh for $\varepsilon = 10^{-3}$: (a) $N = 12$; (b) $N = 24$.

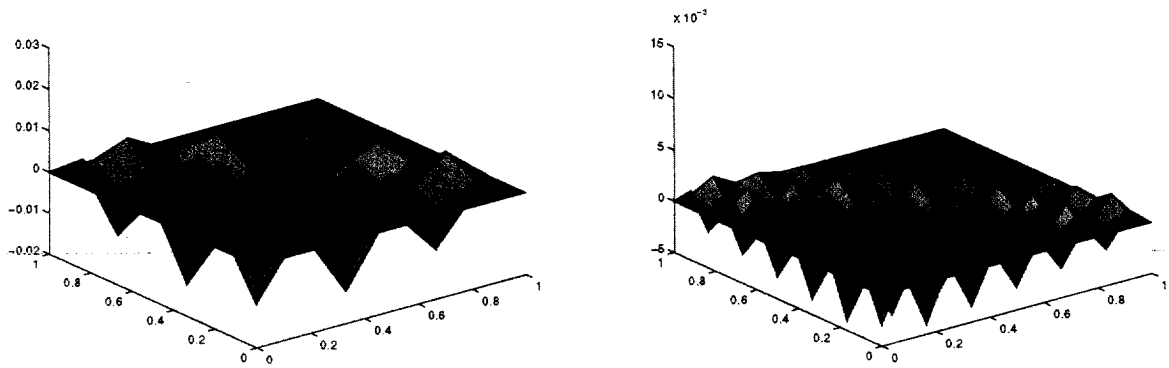

Fig. 2. Example 1: Standard FEM on Shishkin mesh for $\varepsilon = 10^{-5}$: (a) $N = 12$; (b) $N = 24$.

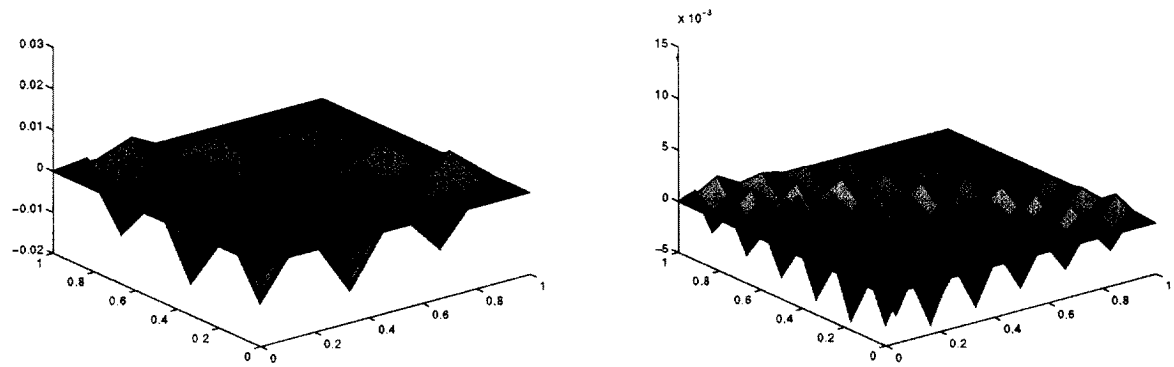

Fig. 3. Example 1: Standard FEM on Shishkin mesh for $\varepsilon = 10^{-7}$: (a) $N = 12$; (b) $N = 24$.

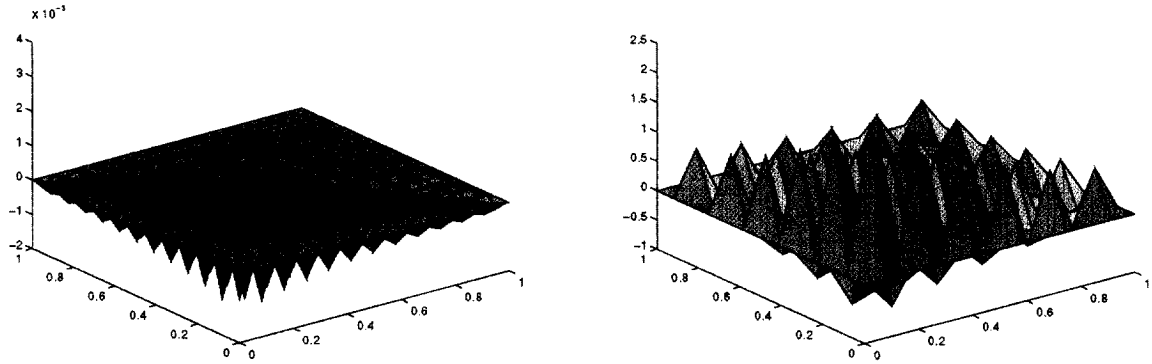

Fig. 4. Example 1: Standard FEM: (a) $N = 48$, $\varepsilon = 10^{-3}$, Shishkin mesh; (b) $N = 12$; $\varepsilon = 10^{-3}$, Uniform mesh.

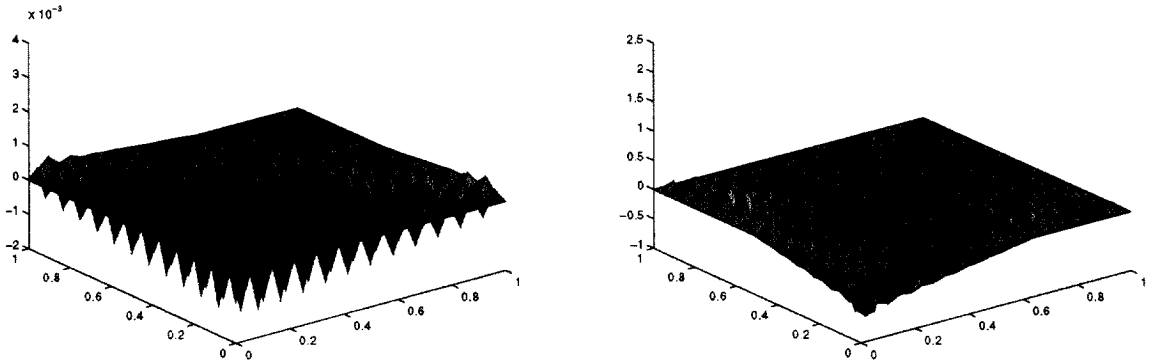

Fig. 5. Example 1: Standard FEM: (a) $N = 48$, $\varepsilon = 10^{-5}$, Shishkin mesh; (b) $N = 24$; $\varepsilon = 10^{-3}$, Uniform mesh.

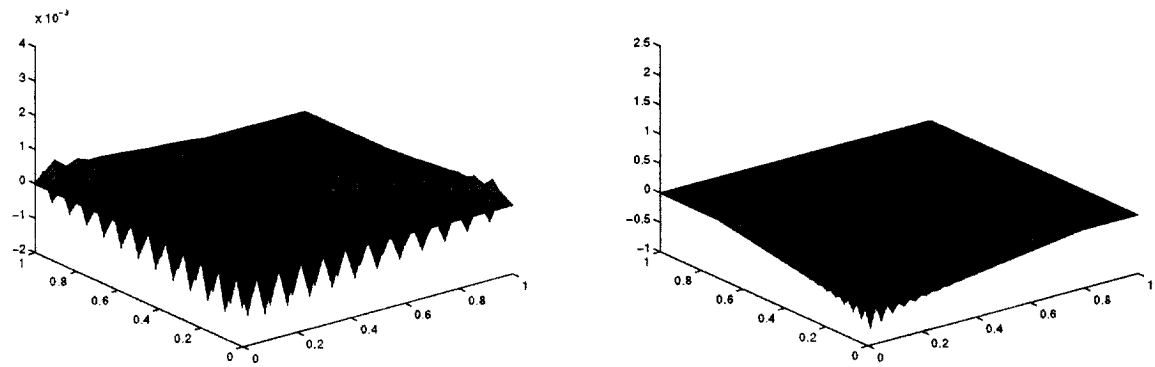

Fig. 6. Example 1: Standard FEM: (a) $N = 48$, $\varepsilon = 10^{-7}$, Shishkin mesh; (b) $N = 48$; $\varepsilon = 10^{-3}$, Uniform mesh.

results in Figs. 4(b)–6(b) for $\varepsilon = 10^{-3}$. When ε becomes smaller, the error amplitude becomes very large. From these results we see that our standard FEM on the Shishkin type mesh performs much better than the classical standard FEM in as far as the error amplitude is concerned. The pollution range is not clear, since the plotting scale is not of the same order of magnitude.

Then, we investigated the streamline diffusion (SD) FEM on our Shishkin type mesh and the standard streamline diffusion FEM [17]. Here, in order to ensure global uniform convergence, we took the diffusion parameter to be $\delta = \varepsilon^2$. Unfortunately, in this case our SD FEM does not improve the standard FEM solution. The pointwise errors are exactly the same as the standard FEM. The reason is that the diffusion parameter δ is too small to have any sizable effect. Then, we tried the popular choice $\delta = 1/N$. The results with the SD FEM on our Shishkin mesh and uniform mesh are presented in Figs. 7–12. Even though our SD FEM on Shishkin

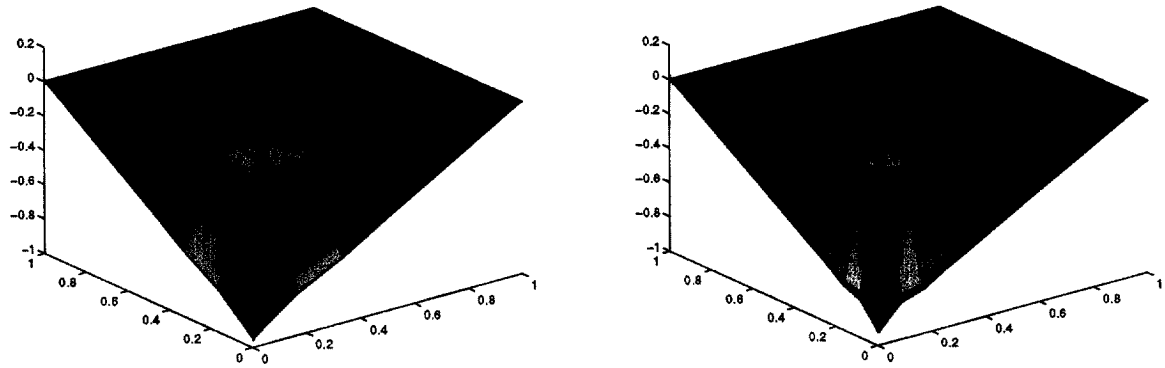

Fig. 7. Example 1: SD FEM on Shishkin mesh for $\varepsilon = 10^{-3}$: (a) $N = 12$; (b) $N = 24$.

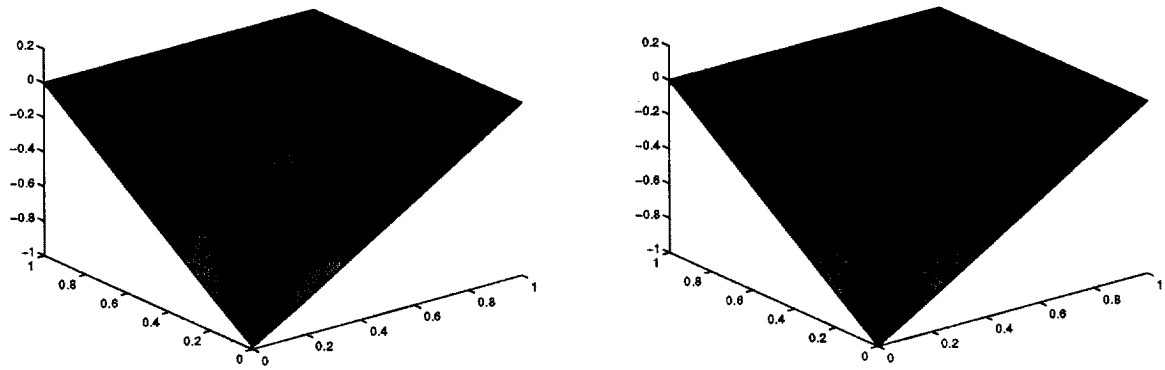

Fig. 8. Example 1: SD FEM on Shishkin mesh for $\varepsilon = 10^{-7}$: (a) $N = 12$; (b) $N = 24$.

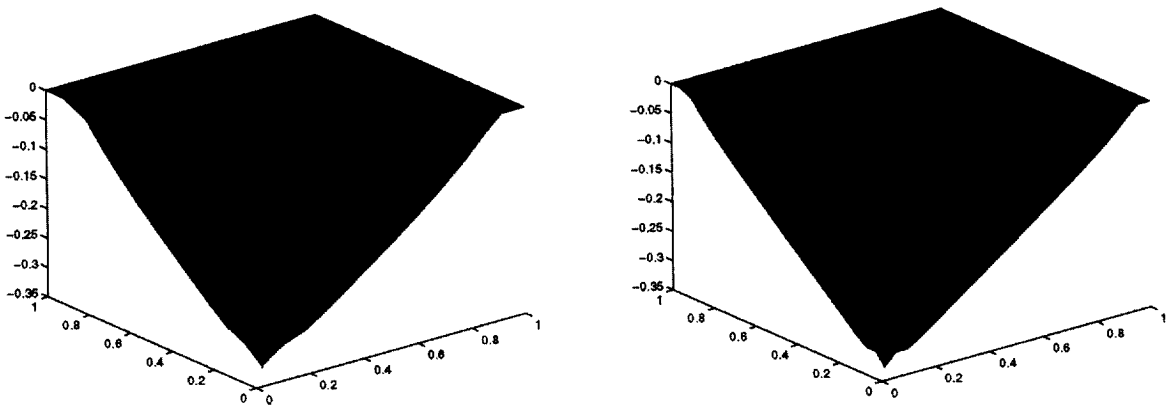

Fig. 9. Example 1: SD FEM on uniform mesh for $\varepsilon = 10^{-3}$: (a) $N = 12$; (b) $N = 24$.

mesh exhibit some oscillations, both methods display a very good local uniform convergence, a fact which was proved recently by Zhou and Rannacher [39], where they also measured accurately the convergence rate for the local pointwise error.

4.2. Example 2

The second example is for the problem given by Eqs. (25), (26) where $b = 1$, $a = 1$ and f is chosen appropriately such that the exact solution is

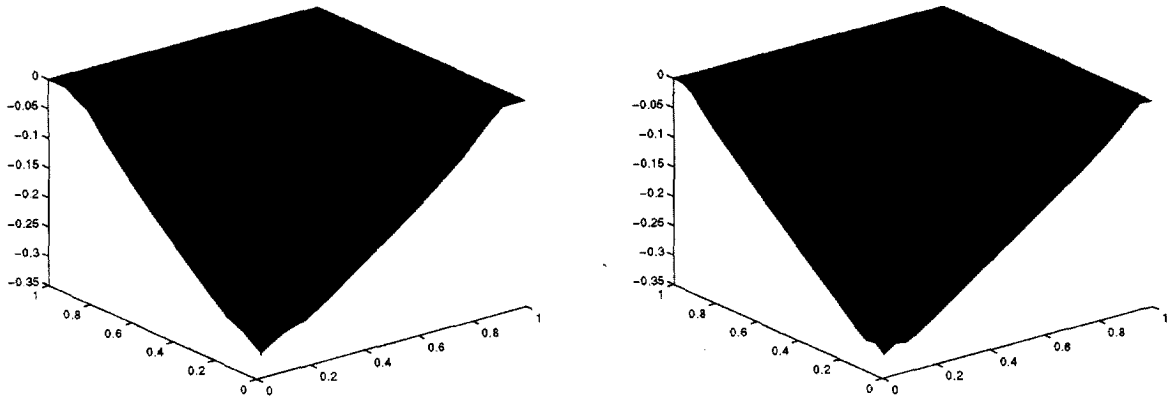

Fig. 10. Example 1: SD FEM on uniform mesh for $\varepsilon = 10^{-7}$: (a) $N = 12$; (b) $N = 24$.

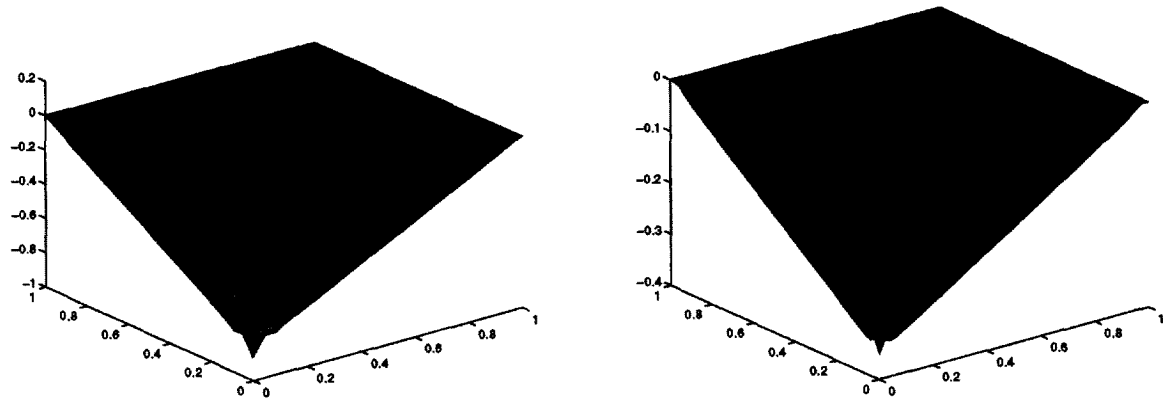

Fig. 11. Example 1: SD FEM for $N = 48$, $\varepsilon = 10^{-3}$: (a) Shishkin mesh; (b) Uniform mesh.

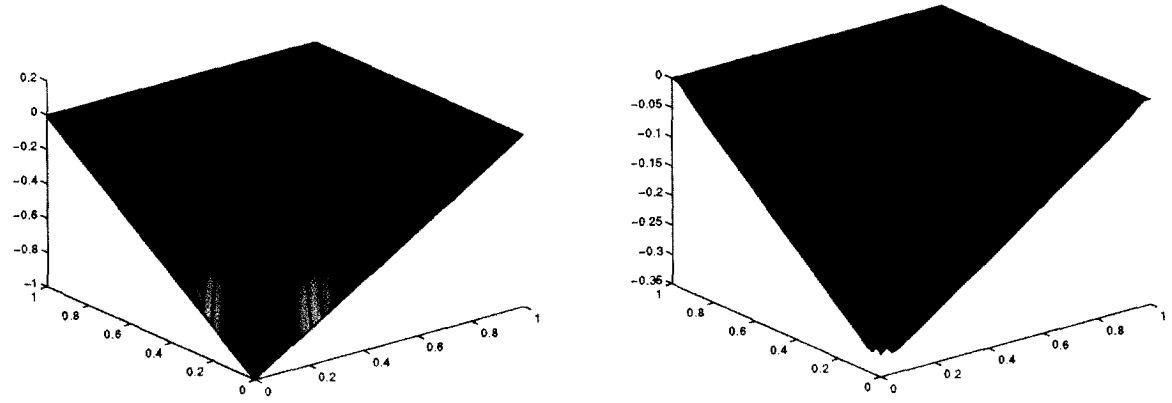

Fig. 12. Example 1: SD FEM for $N = 48$, $\varepsilon = 10^{-7}$: (a) Shishkin mesh; (b) Uniform mesh.

$$u(x, y) = (1 - e^{-x/\varepsilon})(1 - e^{-(1-x)/\varepsilon})(1 - e^{-(1-y)/\varepsilon^2})y.$$

This solution has the typical exponential boundary layers at $x = 0$ and $x = 1$, and it has a parabolic exponential boundary layer at $y = 1$. We choose a bilinear interpolate Πf of f as $\bar{f}$ and $N_x = N_y = N$. The numerical results of our experiments are for values of ε ranging from 10^{-6} to 10^{-2} and for mesh resolutions $N = 12$, 24 and 48, respectively.

First, we tested our standard FEM on Shishkin mesh. The computed L^2 error is provided in Table 4. To see

Table 4
Errors in L^2 norm for Example 2

ε	N		
	12	24	48
1.0D − 02	9.3876868D − 03	2.9110260D − 03	8.7095706D − 04
1.0D − 03	7.7191053D − 03	2.1519899D − 03	5.8664613D − 04
1.0D − 04	7.5300586D − 03	2.0551015D − 03	5.4455535D − 04
1.0D − 05	7.5100947D − 03	2.0453154D − 03	5.4109647D − 04
1.0D − 06	7.5063255D − 03	2.0440796D − 03	5.3940714D − 04

more accurately the convergence order, we provide the computed convergence rate R_ε^N in Table 5. From Table 5, we see that $u^h(x, y)$ approximates $u(x, y)$ uniformly to almost second-order in L^2 norm, which is better than our theoretical analysis. The calculated condition numbers by MATLAB for this problem are provided in Table 6. From these results we see that the condition number is just proportional to ε^{-1}. It is better than the theoretical condition number which should be proportional to ε^{-2}. For the sake of comparison, we performed the computations for standard FEM on the Shishkin mesh and uniform mesh. The pointwise errors $u_h - u$ are plotted in Figs. 13–18 for different ε and N, respectively. We see that the large error also originates from boundary layers, where in our case the exponential boundary layers are located at $x = 0$ and $x = 1$, and the parabolic boundary layer is located at $y = 1$. The error also displays some oscillations and it polluted other regions of the computational domain by propagating from the exponential layer $y = 1$. We conclude that our standard FEM on the Shishkin type mesh performs much better than the classical standard FEM in both the error amplitude and the oscillation frequency.

As for the SD FEM, our SD FEM does not improve the standard FEM as well as in Example 1. Since in order to ensure global uniform convergence, the diffusion parameter δ should satisfy $\delta \leqslant C\varepsilon^n$, $n > 2$ which is too small to have any effect. We tested $\delta = \varepsilon^3$, which yields almost the same solutions as the corresponding standard FEM. Then we tried the popular choice $\delta = 1/N$. The results with the SD FEM on our Shishkin mesh and uniform mesh are presented in Figs. 19–24. They show that no oscillation occurs for either of the SD FEMs. Both methods display very good local uniform convergence, but the SD FEM on our Shishkin type mesh resolves the exponential boundary layers in a much better fashion than SD FEM on the uniform mesh. As N grows larger, the error is dominated only by the parabolic boundary layer.

Table 5
Convergence rates R_ε^N in L^2 norm for Example 2

ε	N	
	12	24
1.0D − 02	1.6892	1.7409
1.0D − 03	1.8428	1.8751
1.0D − 04	1.8735	1.9161
1.0D − 05	1.8765	1.9184
1.0D − 06	1.8767	1.9220

Table 6
Condition numbers for Example 2

ε	N	
	12	24
1.0D − 02	513.0415	973.9048
1.0D − 03	5.6629e + 03	1.1022e + 04
1.0D − 04	5.7141e + 04	1.1148e + 05
1.0D − 05	5.7192e + 05	1.1161e + 06
1.0D − 06	5.7194e + 06	1.1161e + 07

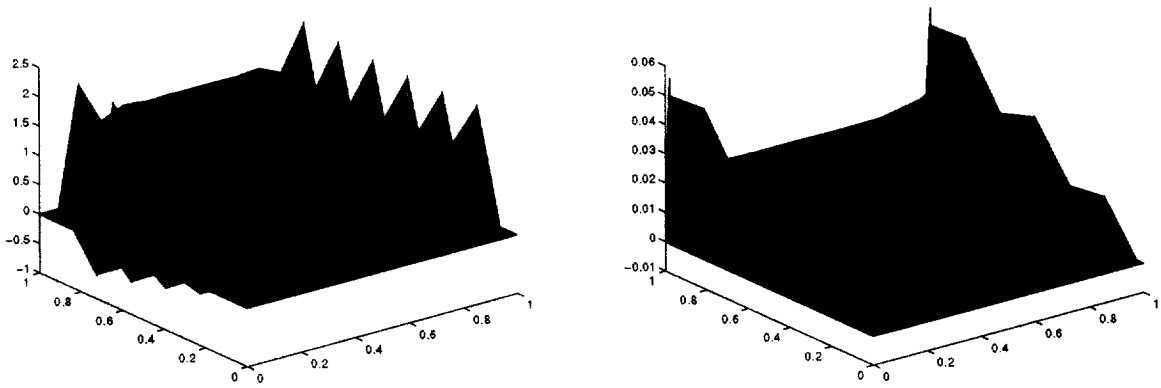

Fig. 13. Example 2: Standard FEM for $N = 12$, $\varepsilon = 10^{-2}$: (a) Uniform mesh; (b) Shishkin mesh.

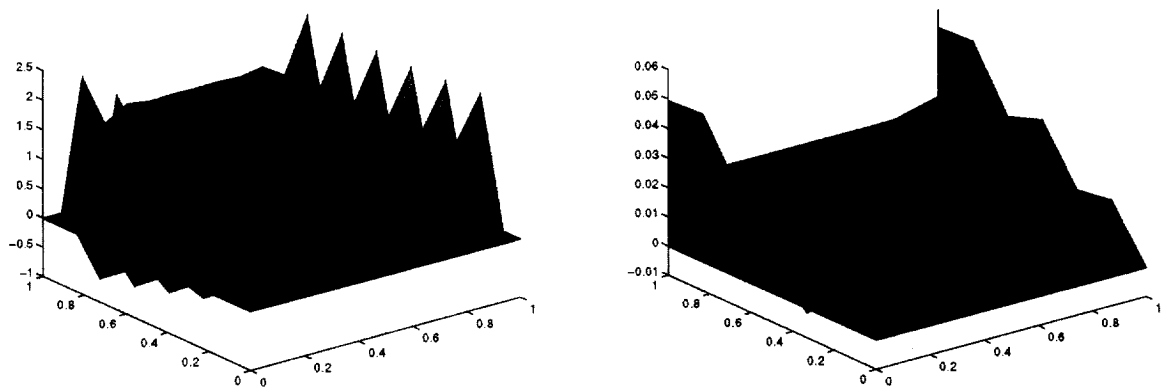

Fig. 14. Example 2: Standard FEM for $N = 12$, $\varepsilon = 10^{-6}$: (a) Uniform mesh; (b) Shishkin mesh.

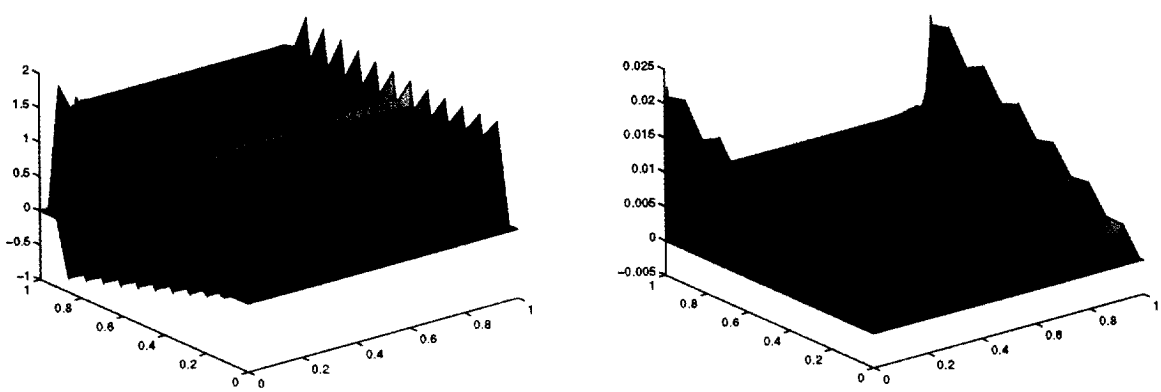

Fig. 15. Example 2: Standard FEM for $N = 24$, $\varepsilon = 10^{-2}$: (a) Uniform mesh; (b) Shishkin mesh.

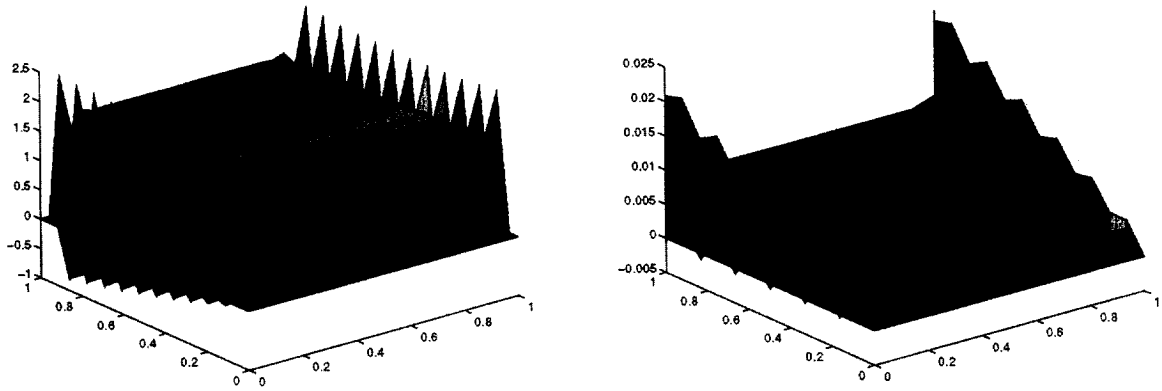

Fig. 16. Example 2: Standard FEM for $N = 24$, $\varepsilon = 10^{-6}$: (a) Uniform mesh; (b) Shishkin mesh.

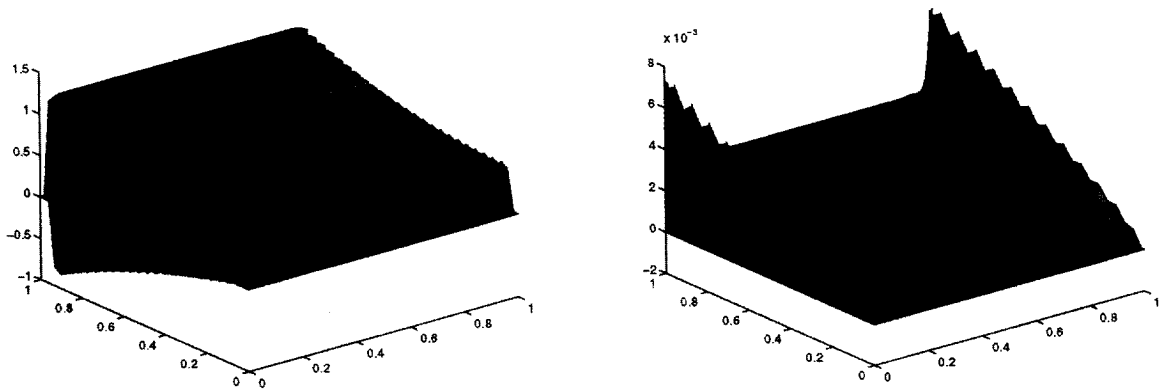

Fig. 17. Example 2: Standard FEM for $N = 48$, $\varepsilon = 10^{-2}$: (a) Uniform mesh; (b) Shishkin mesh.

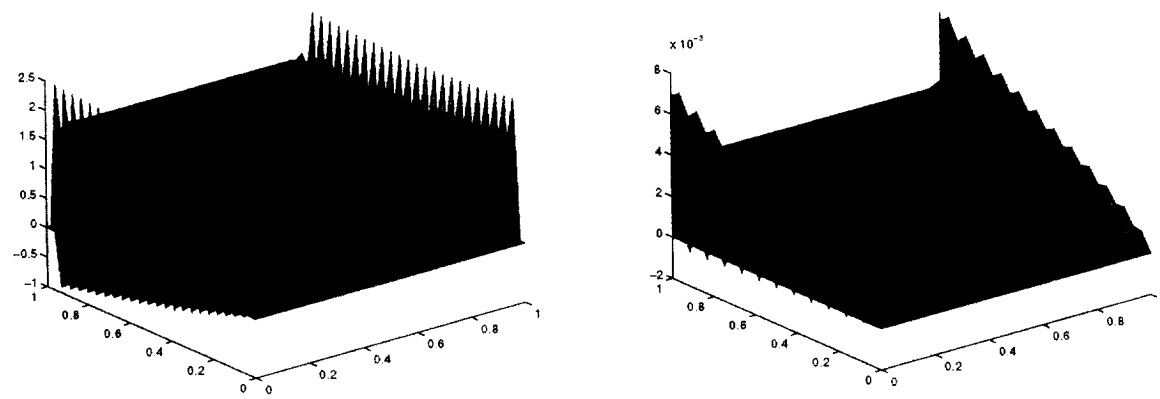

Fig. 18. Example 2: Standard FEM for $N = 48$, $\varepsilon = 10^{-6}$: (a) Uniform mesh; (b) Shishkin mesh.

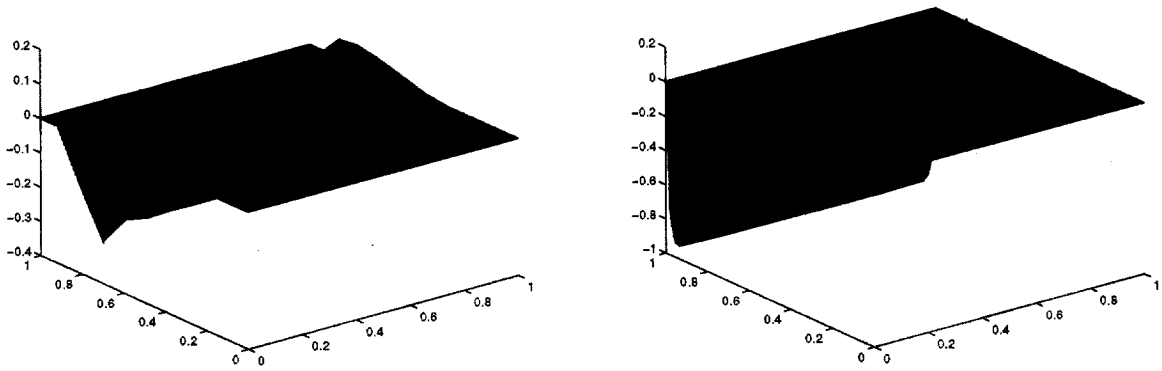

Fig. 19. Example 2: SD FEM for $N = 12$, $\varepsilon = 10^{-2}$: (a) Uniform mesh; (b) Shishkin mesh.

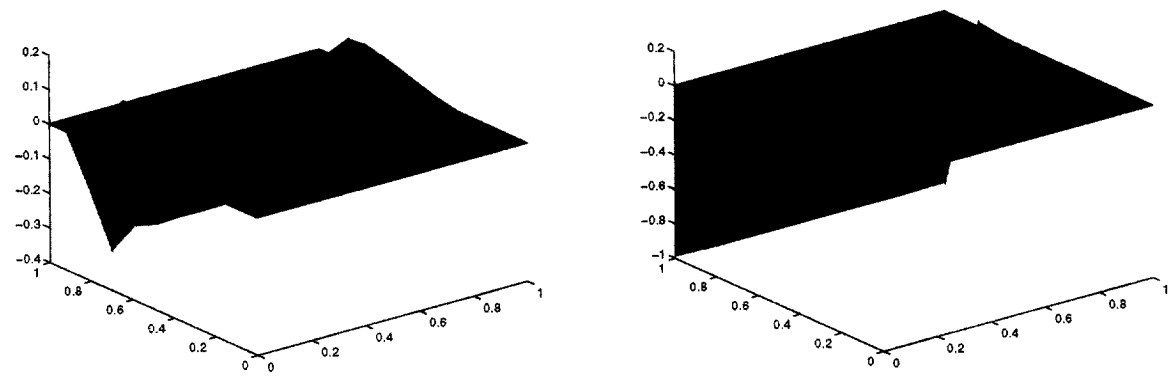

Fig. 20. Example 2: SD FEM for $N = 12$, $\varepsilon = 10^{-6}$: (a) Uniform mesh; (b) Shishkin mesh.

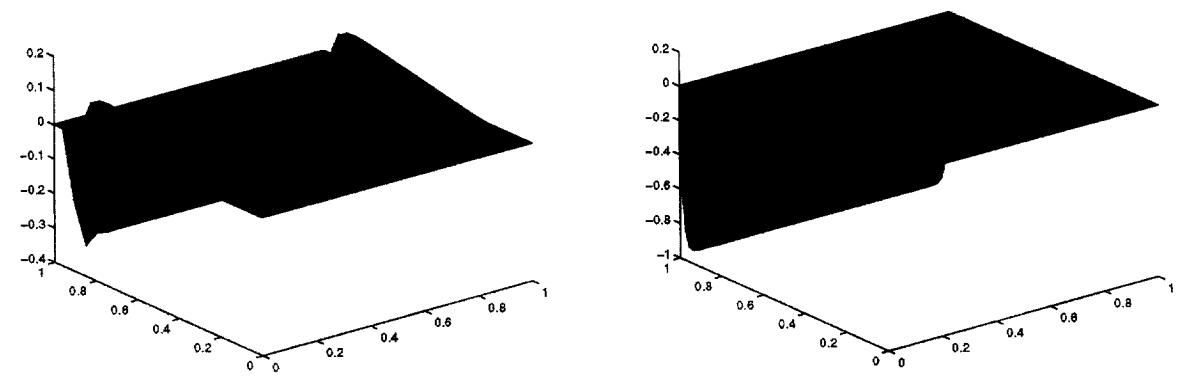

Fig. 21. Example 2: SD FEM for $N = 24$, $\varepsilon = 10^{-2}$: (a) Uniform mesh; (b) Shishkin mesh.

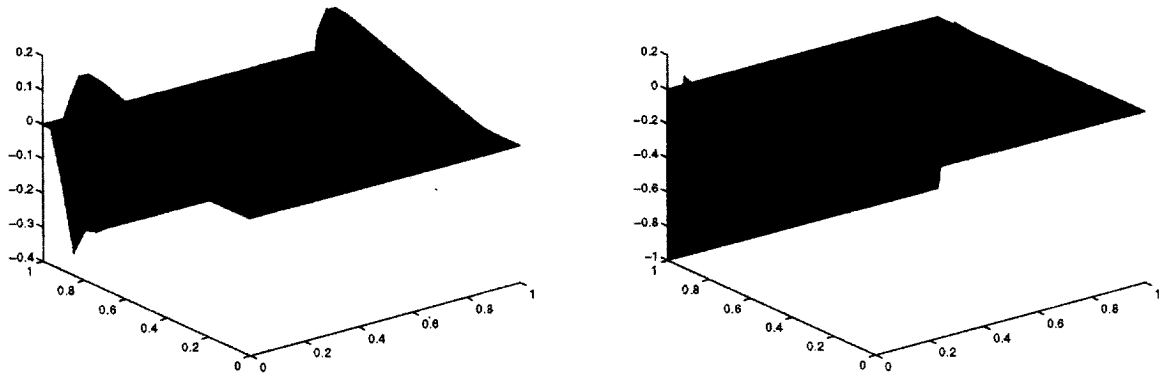

Fig. 22. Example 2: SD FEM for $N = 24$, $\varepsilon = 10^{-6}$: (a) Uniform mesh; (b) Shishkin mesh.

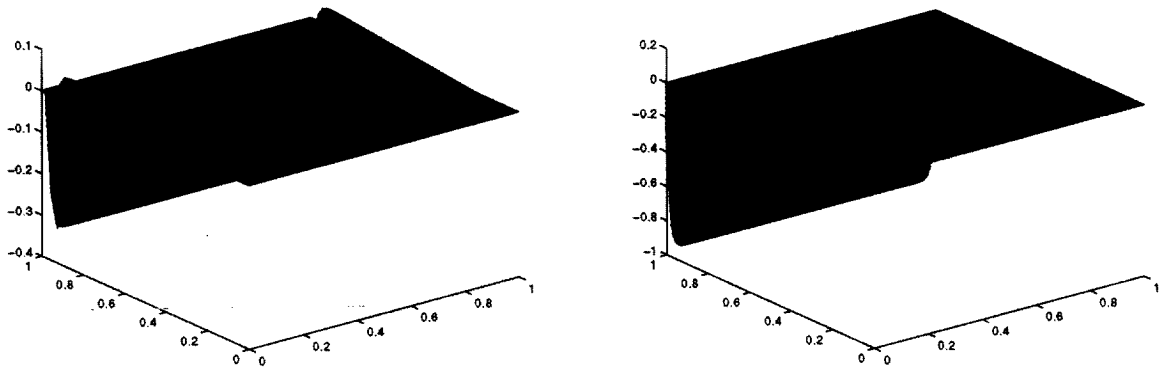

Fig. 23. Example 2: SD FEM for $N = 48$, $\varepsilon = 10^{-2}$: (a) Uniform mesh; (b) Shishkin mesh.

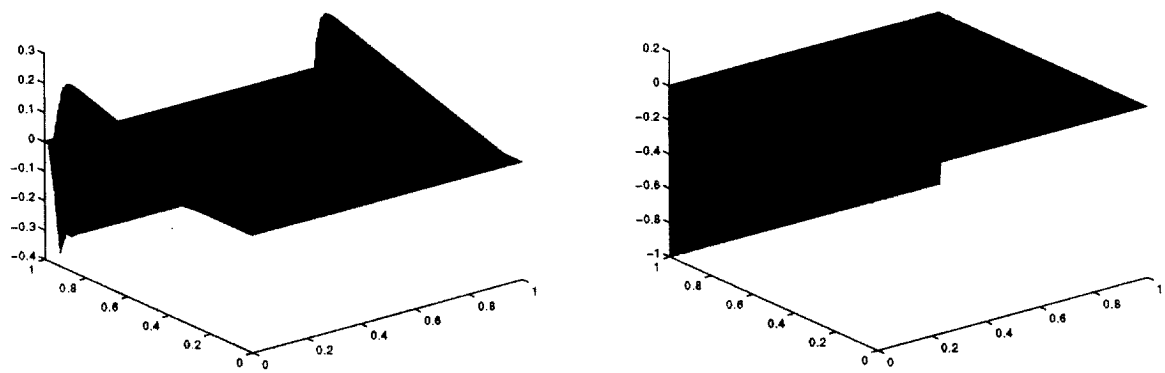

Fig. 24. Example 2: SD FEM for $N = 48$, $\varepsilon = 10^{-6}$: (a) Uniform mesh; (b) Shishkin mesh.

5. Conclusions

Our numerical examples show that both SD FEMs on the Shishkin mesh and the uniform mesh with $\delta = 1/N$ provide a much better control on the error oscillations than the standard FEM. The results also show that both methods display an excellent local uniform convergence, a fact which was proved recently by Zhou and

Rannacher [39] for an almost rectangular mesh, where they also measured accurately the convergence rate for the local pointwise error. For the one space dimension problem, Guo and Stynes [11] recently proved the global uniform convergence for a SD FEM on a Shishkin mesh. But it still remains an open problem [11] whether the global uniform convergence can be retained for SD FEMs in two space dimensions, which is the reason why additional work was dedicated to local error analysis (cf. Johnson et al. [18], Zhou and Rannacher [39] and Wahlbin [37]). Numerical results (see Tables 2 and 5) show that our standard FEM on Shishkin type mesh is GUC in almost second-order in L^2 norm, which is better than our theoretical analysis. At present, it is still unknown if this almost second-order convergence rate can be obtained theoretically for convection-diffusion type problems (it is still unsolved even in one space dimension [19]), or it is just a superconvergence phenomenon [39]. Further investigation is certainly required. Even though our standard FEM on Shishkin type mesh is GUC, it still displays some oscillations around the boundary layers. Other more stable techniques are under development, such as, the stabilized FEM and the techniques developed recently by Franca and Hughes et al. [4,10], along with those discussed in [38, Ch. 12] and Carey and Oden [6, Ch. 5].

Our methods can be applied directly to those nonlinear problems which have uniform asymptotic expansions [35]. Research work on this topic is currently under development. Also, several tests for higher-order FEM on Shishkin mesh are being pursued. Extension to triangular elements and problems with interior layers was investigated by Madden and Stynes [24]. However the theoretical analysis is still missing, and further research work is needed in this area.

Acknowledgments

The authors wish to thank an unknown referee for his useful and incisive suggestions which contributed towards improving the present paper. This research was partly supported by the Air Force Grant E49620-96-1-0172.

References

[1] S. Adjerid, M. Aiffa and J.E. Flaherty, High-order finite element methods for singularly perturbed elliptic and parabolic problems, SIAM J. Appl. Math. 55 (1995) 520–543.
[2] R.E. Bank and M. Benbourenane, The hierarchical basis multigrid method for convection-diffusion equation, Numer. Math. 61 (1992) 7–37.
[3] S.C. Brenner and L.R. Scott, The Mathematical Theory of Finite Element Methods (Springer-Verlag, New York, 1994).
[4] F. Brezzi, L.P. Franca, T.J.R. Hughes and A. Russo, Stabilization techniques and subgrid scales capturing, in: Proceeding of the Conference on the State of the Art in Numerical Analysis, York, England, April, 1996, IMA Conference Series, Oxford University Press, to appear.
[5] V.F. Butuzov, On asymptotics of solutions of singularly perturbed equations of elliptic type in the rectangle, Differential Eqns 11 (1975) 780–787.
[6] G.F. Carey and J.T. Oden, Finite Elements: Fluid Mechanics, Vol. VI (Prentice-Hall, Englewood Cliffs, NJ, 1986).
[7] L. Demkowicz and J.T. Oden, An adaptive characteristic Petrov–Galerkin finite element method for convection-dominated linear and nonlinear parabolic problems in one space variable, J. Comput. Phys. 67 (1986) 188–213.
[8] W. Eckhaus, Asymptotic Analysis of Singular Perturbations (North-Holland, Amsterdam, 1979).
[9] P.A. Farrell, P.W. Hemker and G.I. Shishkin, Discrete approximations for singularly perturbed boundary value problems with parabolic layers, CWI Report 9502, 1995.
[10] L.P. Franca and C. Farhat, Bubble functions prompt unusual stabilized finite element methods, Comput. Methods Appl. Mech. Engrg. 123 (1995) 299–308.
[11] W. Guo and M. Stynes, Pointwise error estimates for a streamline diffusion scheme on a Shishkin mesh for a convection-diffusion problem, IMA J. Numer. Anal. 17 (1997) 29–59.
[12] W. Hackbusch, Multigrid Methods and Applications (Springer-Verlag, Berlin, 1985).
[13] A.F. Hegarty, J.J.H. Miller, E. O'Riordan and G.I. Shishkin, Special meshes for finite difference approximations to an advection-diffusion equation with parabolic layers, J. Comp. Phys. 117 (1995) 47–54.
[14] J.C. Heinrich and O.C. Zienkiewicz, Quadratic finite element schemes for two dimensional convective-transport problems, Int. J. Numer. Methods Engrg. 11 (1977) 1831–44.
[15] X.C. Hu, T.A. Manteuffel, S. MacCormick and T.F. Russell, Accurate discretization for singular perturbations: the one-dimensional case, SIAM J. Numer. Anal. 32 (1995) 83–109.

[16] T.J.R. Hughes, ed., Finite Element Methods for Convection-Dominated Flows, ASME Monograph AMD-34 (ASME, New York, 1979).
[17] C. Johnson, U. Navert and Pitkaranta, Finite element methods for linear hyperbolic problems, Comput. Methods Appl. Mech. Engrg. 45 (1984) 285–312.
[18] C. Johnson, A.H. Schatz and L.B. Wahlbin, Crosswind smear and pointwise errors in streamline diffusion finite element methods, Math. Comput. 49 (1987) 25–38.
[19] R.B. Kellogg and M. Stynes, Optimal approximability of solutions of singularly perturbed two-point boundary value problems, SIAM J. Numer. Anal. (to appear).
[20] J. Kevorkian and J.D. Cole, Multiple Scale and Singular Perturbation Methods (Springer–Verlag, Berlin, 1996).
[21] J. Li, Quasi-optimal uniformly convergent finite element methods for the elliptic boundary layer problem, Comput. Math. Applic. (33)10 (1997) 11–22.
[22] J. Li and I.M. Navon, Uniformly convergent finite element methods for singularly perturbed elliptic boundary value problems I: reaction–diffusion type, Comput. Math. Applic. 35(3) (1998) 57–70.
[23] K.W. Morton, Numerical Solution of Convection-Diffusion Problems (Chapman and Hall, 1996).
[24] N. Madden and M. Stynes, Efficient generation of oriented meshes for solving convection-diffusion problem, Int. J. Numer. Methods Engrg. 40 (1997) 565–576.
[25] R. O'Malley, Singular Perturbations Methods for Ordinary Differential Equations (Springer–Verlag, New York, 1991).
[26] J.J.H. Miller, E. O'Riordan and G.I. Shishkin, Fitted Numerical Methods for Singular Perturbation Problems (World Scientific, Singapore, 1995).
[27] E. O'Riordan and M. Stynes, A globally convergent finite element method for a singularly perturbed elliptic problem in two dimensions, Math. Comput. 57 (1991) 47–62.
[28] H.-G. Roos, A note on the conditioning of upwind schemes on Shishkin meshes, IMA J. Numer. Anal. 16 (1996) 529–538.
[29] H.-G. Roos and M. Stynes, Necessary conditions for uniform convergence of finite difference schemes for convection–diffusion problems with exponential and parabolic layers, Appl. Math. 41 (1996) 269–280.
[30] H.-G. Roos, M. Stynes and L. Tobiska, Numerical Methods for Singularly Perturbed Differential Equations (Springer-Verlag, Berlin, 1996).
[31] Y. Saad, Sparskit: a basic tool kit for sparse matrix computations, Version 2, June 4, 1996.
[32] M.H. Schultz, Spline Analysis (Prentice-Hall, Englewood Cliffs, NJ, 1973).
[33] C. Schwab and M. Suri, The *p* and *hp* versions of the finite element method for problems with boundary layers, Math. Comput. 65 (1996) 1403–1429.
[34] S. Shih and R.B. Kellogg, Asymptotic analysis of a singular perturbation problem, SIAM J. Math. Anal. 18 (1987) 1467–1511.
[35] A.B. Vasil'eva, V.F. Butuzov and L.V. Kalachev, The Boundary Function Method for Singular Perturbation Problems (SIAM, Philadelphia, 1995).
[36] M. Vishik and L. Lyusternik, Regular degeneration and boundary layer for linear differential equations with small parameter multiplying the highest derivatives, Am. Math. Soc. Transl. (2) 20 (1962) 239–364.
[37] L.B. Wahlbin, Local behavior in the finite element method, in: P.G. Ciarlet and J.L. Lions, eds., Handbook of Numerical Analysis, Vol. II, Finite Element Methods (part 1) (North-Holland, Amsterdam, 1991) 355–522.
[38] O.C. Zienkiewicz and R.L. Taylor, The Finite Element Method, Vol. 2 (McGraw–Hill Publ., New York, 1991).
[39] G. Zhou and R. Rannacher, Pointwise superconvergence of the streamline diffusion finite element method, Numer. Methods for PDEs 12 (1996) 123–145.